Energy Conversion and Management 208 (2020) 112595

Contents lists available at ScienceDirect

Energy Conversion and Management

journal homepage: www.elsevier.com/locate/enconman

Comprehensive overview of meta-heuristic algorithm applications on PV cell parameter identification

Bo Yang[a], Jingbo Wang[a], Xiaoshun Zhang[b,*], Tao Yu[c], Wei Yao[d], Hongchun Shu[a], Fang Zeng[a], Liming Sun[e]

[a] Faculty of Electric Power Engineering, Kunming University of Science and Technology, 650500 Kunming, China
[b] College of Engineering, Shantou University, 515063 Shantou, China
[c] College of Electric Power, South China University of Technology, 510640 Guangzhou, China
[d] State Key Laboratory of Advanced Electromagnetic Engineering and Technology, School of Electrical and Electronic Engineering, Huazhong University of Science and Technology, Wuhan 430074, China
[e] Guangzhou ShuimuQinghua Technology CO. LTD, Guangzhou, Guangdong 510898, China

ARTICLE INFO

Keywords:
Meta-heuristic algorithms
Parameter identification
PV cell
Optimization methods

ABSTRACT

Accurate parameter identification is crucial for a precise PV cell modelling and analysis of characteristics of PV systems, while high nonlinearity of output *I-V* curve makes this problem extremely thorny. Hence, a large number of researches have aroused extensive interests in the past few years. Due to the rapid advancement of computer technology and swarm intelligence, various promising meta-heuristic algorithms have been proposed to further accelerate this trend. This paper aims to undertake a comprehensive review on meta-heuristic algorithms and related variants which have been applied on PV cell parameter identification. Particularly, these algorithms are classified into four categories, e.g., biology-based algorithms, physics-based algorithms, sociology-based algorithms and mathematics-based algorithms. Meanwhile, the evaluation criteria and identification performance of each algorithm are thoroughly addressed. Besides, in order to quantitatively evaluate and compare various algorithms, the identified PV parameters including the specific error and the simulated output *I-V* or *P-V* curves are provided at the end of each algorithm. Moreover, a comprehensive summary is also introduced to more specifically guide the readers to grasp and utilize these approaches. Lastly, based on the covered twenty-eight algorithms, conclusion presents some perspectives and recommendations for future development.

1. Introduction

In the past few decades, with the fast depletion of various non-renewable energy resources, e.g., oil, coal and natural gas, as well as the air environment has been seriously polluted, a sustainable energy supply has become a hot and critical issue which has aroused widespread attentions [1–3]. Hence, the exploitation and utilization of renewable energy inevitably play a vital role in future development, in which solar energy acts as one of the most mature and promising option [4–6].

Solar energy can be utilized to generate electrical energy or thermal energy without consuming water/fuel or producing pollutions, which is of great significance in improving the ecological environment. However, the practical application of solar energy still exists difficult obstacles, e.g., low photoelectric conversion efficiency and lack of accuracy in photovoltaic (PV) cell modelling. In particular, precise PV cell modelling is crucial for analyzing and predicting the specific characteristics of PV systems [7]. A series of PV models have been established, such as single diode model (SDM) [8], improved single diode model (ISDM) [9], double diode model (DDM) [10], triple diode model (TDM) [11,12], modified double diode model (MDDM) [10], etc. However, the aforementioned models can hardly maintain a stable and desirable performance in practical applications. Besides, the *I-V* curve provided by manufacturer is only developed under standard test conditions (STC), i.e., $G = 1000\ \mathrm{W/m^2}$ and $T = 25\ ^\circ\mathrm{C}$. Nevertheless, changes in external environment, such as solar irradiation and temperature, will exert a great influence on the output characteristics of PV cells. Furthermore, the inherent property of PV cells, such as high nonlinearity of PV characteristics, also result in the precise PV cell modelling to be extremely thorny.

* Corresponding author.
E-mail address: xszhang1990@sina.cn (X. Zhang).

https://doi.org/10.1016/j.enconman.2020.112595
Received 9 September 2019; Received in revised form 19 January 2020; Accepted 9 February 2020
Available online 20 February 2020
0196-8904/

Nomenclature

Variables

I_{ph}	photocurrent, A
I_d, I_{d1}, I_{d2}	diode's currents, A
I_0, I_{01}, I_{02}, I_{03}	diode's reverse saturation currents, A
R_s	series resistor, Ω
R_{sh}	shunt resistor, Ω
a, a_1, a_2, a_3	diode's ideality factors

Abbreviations

PV	photovoltaic
SDM	single diode model
DDM	double diode model
TDM	triple diode model
RMSE	root mean square error
NRMSE	normalized root mean square error
RMSD	root mean square deviation
NRMSD	normalized root mean square deviation
MAE	mean absolute error
MAEP	mean absolute error in power
MBE	mean bias error
AE	absolute error
IAE	individual absolute error
RE	relative error
MRE	mean relative error
MAPE	mean absolute percentage error
MABE	mean absolute bias error
STC	standard test conditions
MPPT	maximum power point tracking
E.P.	extracted parameters
N.S.	not specified
N.I.	not identified
A.M.	analytical method
G	irradiation, W/m^2
T	temperature, °C
I-V	current–voltage
P-V	power-voltage
GA	genetic algorithm
DE	differential evolution
ABSO	artificial bee swarm optimization
ABC	artificial bee colony
WOA	whale algorithm
IAIO	improved antlion optimizer
BBO	biogeography based optimization
CS	cuckoo search
BMO	bird mating optimization
FPA	flower pollination algorithm
GWO	grey wolf optimization
BFA	bacterial foraging algorithm
AIS	artificial immune system
SSA	salp swarm algorithm
PSO	particle swarm optimization
MPCOA	mutative scale parallel chaos optimization algorithm
SA	simulated annealing
FWA	fireworks algorithm
WDO	wind driven optimization
ER-WCA	evaporation rate based water cycle algorithm
LCOA	Lozi map-based chaotic optimization algorithm
HS	harmony search
TLBO	teaching learning based optimization
ICA	imperialist competitive algorithm
MLBSA	multiple learning backtracking search algorithm
PS	pattern search
SCE	shuffled complex evolution
JAYA	JAYA algorithm
PSC	partial shading conditions

In general, precise PV cell modelling is mainly based on accurate parameter identification. Besides, parameter identification is of great importance in simulation, performance evaluation, optimization design and real-time control of PV systems [13,14]. Additionally, it can also provide meaningful guidance for application design in terms of battery manufacturing, photoelectric conversion enhancement and maximum power point tracking (MPPT) [15,16]. Since the significance of parameter identification has received ever-increasing interests, an enormous variety of studies are undertaken to develop feasible and practical methods to solve such problem.

Consequently, numerous methods are proposed to crack this hard nut [17–19], while these strategies can be mainly classified into two categories [20–22], i.e., analytical methods [23–25] and meta-heuristic algorithms [26,27]. The analytical approaches utilize a series of complex mathematical equations to extract these parameters [28–30]. Among which reference [31] combined statistical methods with analytical methods to effectively identify the unknown parameters. However, such methods also have distinct disadvantages, e.g., large calculation burden and complex mathematical operations, which require an enormous amount of time and computation costs [17].

On the other hand, with the development of computer and swarm intelligence, various meta-heuristic algorithms have achieved extensive applications, especially in highly nonlinear and complex optimization problems [32,33]. One of their most prominent advantages is that they can do not require an accurate mathematical model of the studied system [34], such that the computational burden can be greatly reduced. Thus far, numerous meta-heuristic algorithms have been reported for PV cell parameter identification in an astonishing speed [35]. To provide a state-of-the-art introduction of these studies, this paper undertakes a comprehensive review of twenty-eight meta-heuristic algorithms for PV cell parameter identification. Meanwhile, these algorithms are divided into four groups, i.e., biology-based algorithms, physics-based algorithms, sociology-based algorithms and mathematics-based algorithms. In particular, their main principle with the related variants, advantages and disadvantages are also thoroughly addressed.

The rest of this paper is organized as follows: the mathematical modelling of PV cell is demonstrated in Section 2. A series of evaluation criteria are illustrated in Section 3. Various meta-heuristic algorithms are introduced in Section 4. Section 5 makes a comprehensive summary and comparison of different meta-heuristic algorithms. Lastly, conclusions are provided in Section 6.

2. PV cell modelling

The establishment of PV cell model is the essential part for analyzing the output characteristics of PV systems. Only an accurate fitting of output *I-V* and *P-V* curves of PV cells can reliably evaluate and predict the performance of PV systems, which is highly relied on the accurate identification of the required DC parameters from PV cell model.

2.1. PV devices

During the past few decades, crystalline silicon solar cells are mainly applied on the utilization of solar energy in large scale, which are mainly classified into three types, i.e., mono-crystalline silicon, multi-crystalline silicon and thin film, respectively [35]. Besides, it is noteworthy that high concentrating photovoltaic (HCPV) technique [36] has been utilized in grid-connected power plants, while the application of Fresnel lenses in HCPV system can significantly reduce the manufacturing cost. Moreover, HCPV system also owns high conversion efficiency which has been verified by practical engineering implementation. Particularly, Table 1 undertake a systematic summary of the aforementioned PV devices.

2.2. Mathematical modelling

This section aims to undertake a brief review on several widely applied and representative PV models, e.g., SDM, DDM, and TDM. Particularly, the main structures of these models are basically the same which mainly consist of an ideal constant current sourceI_{ph}, a series resistorR_s, and a shunt resistor R_{sh}, while the main difference is the number of parallel diodes. In order to more systematically and clearly compare these models, a comprehensive summary is tabulated in Table 2.

As illustrated in Table 2, I_{sh} means the current passing through the shunt resistor R_{sh}; $q = 1.6 \times 10^{-19}$C represents the electron charge; while the thermal voltageV_T is given as

$$V_T = \frac{N_s KT}{q} \tag{1}$$

whereN_s means the number of PV cells connected in series in PV panel (For a single PV cell, $N_s = 1$); T represents the cell temperature; and K= 1.38×10^{-23}J/K denotes the Boltzmann constant, respectively.

Moreover, an additional Table 3 is provided to more explicitly demonstrate and compare the characteristics of the three aforementioned PV models in the revised manuscript. In particular, the advantages and disadvantages, and suitable situation for practical working condition for each model are specifically addressed.

3. Evaluation Criteria

For the sake of quantitatively evaluating the performance of various parameter identification approaches, a series of evaluation criteria and objective functions are proposed to effectively verify whether the algorithms can obtain desirable results. Particularly, the representative equations, features, and variables utilized in various criteria are summarized in Table 4. Basically, the utilization of absolute value in calculation is to avoid negative values while the formulas with square can more precisely output the results.

4. Meta-heuristic algorithms for PV cell parameter identification

With the rapid advancement of computer, meta-heuristic algorithms have been greatly enriched and extensively utilized over the recent decades. Started with genetic algorithm (GA) [67–69], numerous meta-heuristic algorithms have been developed and popularly adopted to deal with different practical optimization issues. In general, meta-heuristic algorithms can effectively improve the calculation accuracy, reduce the computation burden, and acquire a high-quality optimum when solving complex optimization problems [33]. In this section, twenty-eight meta-heuristic algorithms are introduced and classified into four categories, i.e., biology-based algorithms, physics-based algorithms, sociology-based algorithms and mathematics-based algorithms. Meanwhile, the basic theory of various meta-heuristic algorithms will be introduced, together with the introduction of their hybrid or variants. Besides, the basic electrical specification from datasheet of three widely applied PV cell/module is demonstrated in Table 5 for better understanding.

4.1. Biology-based algorithms

4.1.1. Genetic algorithm

GA is a biology-based algorithm inspired by the evolution mechanism in nature [69], which mainly consists of three steps, i.e., selection, crossover and mutation [73,74], while its flowchart is demonstrated in Fig. 1.

For the sake of further enhancing the performance of traditional GA to better apply it on parameter identification, several improved versions are proposed. In order to lessen the computation burden of GA, a hybrid algorithm (GA + NR) was proposed to extract two parameters in [75], in which NR represents Newton Raphson method. Moreover, adaptive GA (AGA) can effectively enhance computation efficiency and alleviate the local minimization, in which adaptive genetic parameters, i.e., crossover and mutation probability are introduced [76]. Besides, the simulation results demonstrate that AGA can accurately fit the curves under different irradiation conditions compared with traditional GA methods.

4.1.2. Differential evolution

DE mainly consists of four phases, e.g., initialization, mutation, crossover, and selection [35,77]. Recently, many adaptive/improved DE variants have been developed, such as improved adaptive DE (IADE) [78], repaired adaptive DE (R_{cr}-IJADE) [79], penalty based DE (P-DE) [80], improved DE algorithm with adaptive mutation per iteration algorithm (DEAM) [81], onlooker-ranking-based adaptive DE (OR_{cr}-IJADE) [82]. For instance, the crossover rate and mutation factor are adaptively controlled in R_{cr}-IJADE, such that the crossover operation can be expressed as

$$U_{ji,G} = b_{ij} V_{ji,G} + (1 - b_{ij})\cdot X_{i,G} \tag{2}$$

$$C_{r2} = \frac{\sum_{j=1}^{D} b_{ij}}{D} \tag{3}$$

where C_{r2} is the repaired crossover rate; $V_{ji,G}$ denotes the resultant vector; $U_{ji,G}$ means the trial vector; b_{ij} denotes a binary string produced for each target vector $X_{i,G}$; and D represents the number of decision variables, respectively.

All the variants mentioned before have been applied on PV cell

Table 1
Features of four PV devices.

Devices	Photoelectric conversion efficiency Highest in labs	Advantages	Disadvantages
Mono-crystalline silicon [37–39]	25.6%	a) high conversion efficiency; b) low maintenance cost.	a) high costs; b) complicated manufacturing.
Poly-crystalline silicon [40–42]	22.3%	a) relatively high conversion efficiency; b) low costs.	a) limited supply; b) complicated manufacturing.
Thin film [43–45]	23.3%	a) low costs which is beneficial for mass production.	a) low stability; b) medium–low conversion efficiency.
HCPV system [36,46]	28%	a) low costs; b) the highest conversion efficiency or total energy production.	a) require accurate solar tracking to maintain high performance.

Table 2
Basic introduction of three PV cell models.

Diode model	Model drawing	Output *I-V* equation	Identified parameters
SDM [8,47]	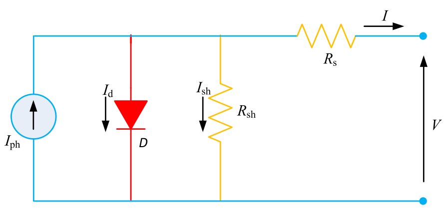	$I = I_{ph} - I_0\left[\exp\left(\frac{q(V+IR_S)}{aKT}\right) - 1\right] - \frac{V+IR_S}{R_{sh}}$	I_{ph}, I_0, R_s, R_{sh}, and$a$
DDM [48,49]	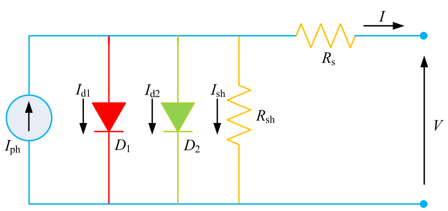	$I = I_{ph} - I_{01}\left[\exp\left(\frac{q(V+IR_S)}{a_1V_T}\right) - 1\right] - I_{02}\left[\exp\left(\frac{q(V+IR_S)}{a_2V_T}\right) - 1\right] - \frac{V+IR_S}{R_{sh}}$	I_{ph}, I_{01}, I_{02}, R_s, R_{sh}, a_1, and a_2
TDM [11,12]	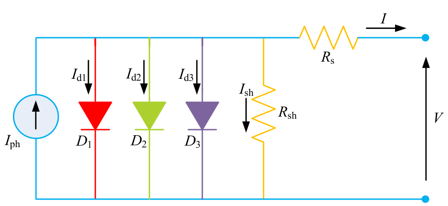	$I = I_{ph} - I_{01}\left[\exp\left(\frac{q(V+IR_{S0}(1+KI))}{a_1V_T}\right) - 1\right] - I_{02}\left[\exp\left(\frac{q(V+IR_{S0}(1+KI))}{a_2V_T}\right) - 1\right] - I_{03}$ $\left[\exp\left(\frac{q(V+IR_{S0}(1+KI))}{a_3V_T}\right) - 1\right] - \frac{V+IR_{S0}(1+KI)}{R_{sh}}$	I_{ph}, I_{01}, I_{02}, I_{03}, R_s, R_{sh}, a_1, a_2, and a_3

Table 3
Comparison of three PV cell models.

PV model	Advantages	Disadvantages	Suitable situation
SDM [50–52]	a) simple control structure; b) low circuit complexity and implementation cost; c) easy hardware implementation.	a) poor accuracy with high irregularity in output characteristics; b) lack of stable performance under PSC; c) less efficient replicate precise *I-V* curve.	a) the most widely used PV model due to its simplicity; b) suitable for the PV systems which require fast response and relatively low manufacturing cost.
DDM [50,53–55]	a) high curve fitting accuracy; b) satisfactory performance under STC; c) easy hardware implementation.	a) slightly high complexity and implementation cost; b) low circuit complexity.	a) practical applications which require accurate output *I-V* characteristics, especially at low irradiation level; b) need to adapt to varying environment conditions.
TDM [11,12,56]	a) can clearly determine the various current components of PV cells; b) highest curve fitting accuracy.	a) high complexity in modelling; b) long execution time; c) complex hardware implementation	a) replicate the output *I-V* characteristics of large area industrial silicon solar cells; b) need to describe complicated physical behaviour of multi-crystalline silicon solar cells.

parameter identification, in which $\mathrm{OR_{cr}}$-IJADE can achieve the most satisfactory results.

4.1.3. Artificial bee swarm optimization

Artificial bee swarm optimization (ABSO) strategy mainly mimics the nectar collecting and processing behavior of bees [83]. Basically, the bees are classified into two groups, i.e., onlookers and scouts, while some onlooker bees are selected as elite bees which can better exploit potential optimal solutions. Particularly, the number of elite bees plays a crucial role in the optimal performance of ABSO. In general, ABSO can acquire a more desirable performance in DDM, which outperforms PSO, GA and SA in validations, but lacks rapid convergence. For the purpose of verifying the practical performance of ABSO, the PV cell parameter identification results are illustrated in Table 6.

4.1.4. Artificial bee colony

Artificial bee colony (ABC) optimization approach mainly replicates the intelligent food searching behavior of bees [84,85], in which different bees modify their positions via different types of paths [86,87]. In particular, for the sake of more efficiently balancing the local exploitation and global exploration, a new hybrid strategy named teaching learning artificial bee colony (TLABC) algorithm is proposed [88]. In TLABC, the new food sources can be updated through teaching-based strategy, as follows:

$$u_s = \begin{cases} x_s + r\cdot(x_s - x_j), & \text{if}\, f(x_s) \leqslant f(x_j) \\ x_s + r\cdot(x_j - x_s), & \text{if}\, f(x_j) \leqslant f(x_s) \end{cases} \tag{4}$$

where x_s represents the previous food source, $j\in\{1, 2, \cdots, NP\}$ and $j\neq s$; u_s denotes the updated food source; r means a random vector uniformly distributed in [0,1]; and NP represents the population size, respectively.

Both ABC and TLABC have been applied on PV cell parameter identification, while the simulation results are demonstrated in Table 7.

4.1.5. Whale optimization algorithm

Whale optimization algorithm (WOA) mainly replicates the unique hunting mechanism of humpback whales, i.e., bubble-net hunting strategy [89–91]. Besides, the humpback whales also utilize random searching strategy to search preys through exchanging information with other whales, as follows [92]:

$$D = |C\cdot X_r - X_t| \tag{5}$$

$$X_{t+1} = X_r - A\cdot D \tag{6}$$

where X_r represents the position of a random whale; D means the

Table 4
Criteria summary.

Criteria	Representative equation	Features		Variables	
		Absolute value	Square (including variance and standard deviation)	Current (I)	Power (P)
Root mean square error (RMSE) [57]	$\mathrm{RMSE} = \sqrt{\frac{1}{N}\sum_{i=1}^{N}(f_i(V, I, x))^2}$		✓	✓	
Normalized root mean square error (NRMSE) [58,46]	$\mathrm{NRMSE} = \frac{\sqrt{\frac{1}{N}\sum_{i=1}^{N}(I_{\mathrm{exp}} - I_{\mathrm{sim}})^2}}{\sqrt{\frac{1}{N}\sum_{i=1}^{N}I_{\mathrm{exp}}^2}}$		✓	✓	
Root mean square deviation (RMSD) [59]	$\mathrm{RMSD} = \sqrt{\frac{\sum_{i=1}^{N_{\mathrm{curve}}}(I_{\mathrm{i}} - I_{\mathrm{j}})^2}{N_{\mathrm{curve}}}}$		✓	✓	
Normalized root mean square deviation (NRMSD) [59]	$\mathrm{NRMSD} = \frac{\mathrm{RMSD}}{I_{\mathrm{sc}}}$		✓	✓	
Mean absolute error (MAE) [60]	$\mathrm{MAE} = \frac{1}{N}\sum_{i=1}^{N}\lvert I_i - I(V_i, a)\rvert$	✓		✓	
Mean absolute error (MAEP) [59]	$\mathrm{MAEP} = \frac{\sum\lvert P_{\mathrm{curve}} - P_{\mathrm{model}}\rvert}{N_{\mathrm{curve}}}$	✓			✓
Mean bias error (MBE) [61]	$\mathrm{MBE} = \frac{1}{N}\sum_{i=1}^{N}[I_i - I(V_i, a)]^2$		✓	✓	
Absolute error (AE) [62]	$\mathrm{AE} = \lvert I_{\mathrm{mes}} - I_{\mathrm{cal}}\rvert$	✓		✓	
Individual absolute error (IAE) [63]	$\mathrm{IAE} = \lvert I_{\mathrm{pvmes},i} - f(I_{\mathrm{pv}}, V_{\mathrm{pv}}, \theta)_i\rvert$	✓		✓	
Relative error (RE) [64]	$\mathrm{RE} = \left\lvert\frac{I_{\mathrm{mes}} - I_{\mathrm{cal}}}{I_{\mathrm{mes}}}\right\rvert$	✓		✓	
Mean relative error (MRE) [65]	$\mathrm{MRE} = \frac{1}{N}\sum_{i=1}^{N}RE_i$	✓		✓	
Mean absolute percentage error (MAPE) [66]	$\mathrm{MAPE} = \frac{1}{N}\sum_{i=1}^{N}\left\lvert\frac{I_{\mathrm{identi}} - I_{\mathrm{target}}}{I_{\mathrm{target}}}\right\rvert$	✓		✓	
Mean absolute bias error (MABE) [66]	$\mathrm{MABE} = \frac{\sum_{i=1}^{N}(I_{\mathrm{identi}} - I_{\mathrm{target}})^2}{\sum_{i=1}^{N}(I_{\mathrm{identi}} - I_{\mathrm{mean}})^2}$		✓	✓	

Table 5
Basic electrical specification of PV cell/module.

Parameter	57 mm R.T.C. France solar cell [70]	KC200GT PV module [71]	SM55 PV cell [72]
Type	Poly-crystalline	Poly-crystalline	Mono-crystalline
Maximum Power (P_{mpp}) (W)	0.3101	200	55
Voltage at MPP (V_{mpp}) (V)	0.4507	26.3	17.4
Current at MPP (I_{mpp}) (A)	0.6880	7.61	3.15
Open Circuit Voltage (V_{oc}) (V)	0.5728	32.9	21.7
Short Circuit Current (I_{sc}) (A)	0.7603	8.21	3.45
Temperature coefficient of I_{sc} (A/°C)	0.035	0.00318	0.04
Number of series cells (N_s)	1	54	36

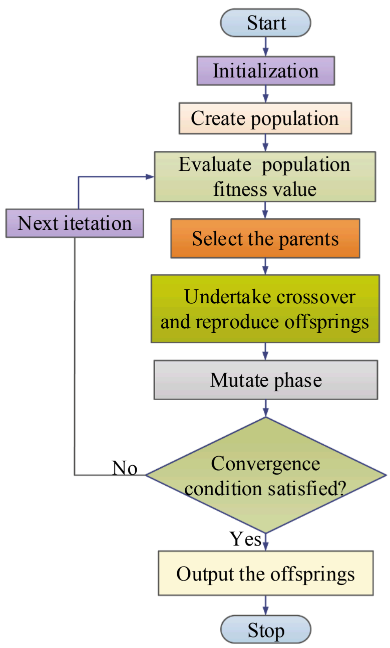

Fig. 1. Flowchart for GA method.

distance between whale and prey; t means the current iteration number; while A and C represent coefficient vectors, if $|A| \geqslant 1$, the position of a whale will be updated according to a random whale.

To remedy the drawbacks of original WOA, improved WOA (IWOA) [93] and chaotic WOA (CWOA) [94] are proposed to enhance the convergence speed and global searching quality. Besides, modified WOA (MWOA) [95] can efficiently enhance the local exploitation ability and solution accuracy. Lastly, Table 8 demonstrates the results obtained by WOA variants for PV cell parameter identification.

4.1.6. Improved ant lion optimizer

Improved antlion optimizer (IAIO) algorithm mainly imitates the hunting behavior of ant lions [96]. Compared with original antlion optimizer (AIO), chaotic sequence and position updating formula of PSO algorithm are introduced in IAIO to avoid premature convergence and enhance searching efficiency. Basically, the chaotic sequence is generated through combining a random sequence x while all elements in the sequence are in the range of [0,1], as follows:

$$L_{i,j} = 4x_{i,j}^2 - 3x_{i,j} \tag{7}$$

where $x_{i,j}$ may be ants position or ant lions position. The sequence is efficient only the initial value is not 0, then its value will be sent back to the solution space through mapping.

Fig. 2 demonstrates the output *I-V* curve acquired under various methods and solar irradiation [96].

4.1.7. Biogeography based optimization

Biogeography based optimization (BBO) is a global searching strategy based on the phenomenon of island biogeography, which has two operators called migration and mutation [97,98]. To overcome the shortcomings of conventional BBO, BBO-M strategy incorporates the mutation strategy from DE into the original migration of BBO [99] to effectively enhance the exploitation capability. Moreover, chaos theory is also employed in BBO to adjust the solution in mutation, which can effectively avoid premature convergence. Meanwhile, the mutation with chaos theory is a mild regulation that is different from the random mutation, which can easily find an optimum.

In particular, the simulated results acquired by BBO-M when applied on PV cell parameter identification are tabulated in Table 9.

4.1.8. Cuckoo search

Cuckoo search (CS) algorithm imitates the reproduction strategy called brood parasitism of cuckoos, in which Levy flights mechanism is adopted rather than simple random walk [100,101]. Besides, three idealized principles are set to guide the operation of this algorithm, thus the new generated solution by Lévy flights rules can be expressed as [102]

$$X_i^{t+1} = X_i^t + \alpha \oplus \text{Levy}(\beta) \tag{8}$$

where X_i represents the position of the ith egg; t represents the generation number; α means the step size parameter depending on the scales of problem; $\oplus$ represents entry-wise multiplications; and β represent the Lévy flight exponent, respectively.

Furthermore, in order to improve the accuracy and reliability of original CS, a new hybrid version of CS called biogeography-based heterogeneous cuckoo search (BHCS) algorithm is proposed in [103]. To this end, the specific performance of two methods on parameter identification are demonstrated in Table 10.

Table 6
PV cell parameter identification using ABSO (57 mm R.T.C. France solar cell).

ABSO	SDM	$R_s(\Omega)$	$R_{sh}(\Omega)$	I_{ph}(A)	$I_0(\mu A)$	a		
	Range Set	0–0.5	0–100	0–1	0–1	1–2		
	E.P.	0.03659	52.2903	0.7608	0.30623	1.4758		
	RMSE	9.9124E-04						
	DDM	$R_s(\Omega)$	$R_{sh}(\Omega)$	I_{ph}(A)	$I_{01}(\mu A)$	a_1	$I_{02}(\mu A)$	a_2
	Range Set	0–0.5	0–100	0–1	0–1	1–2	0–1	1–2
	E.P.	0.03657	54.6219	0.7608	0.26713	1.4651	0.3819	1.9815
	RMSE	9.8344E-04						

Table 7
PV cell parameter identification using ABC and its variant (57 mm R.T.C. France solar cell).

ABC	SDM	$R_s(\Omega)$	$R_{sh}(\Omega)$	I_{ph}(A)	$I_0(\mu A)$	a		
	Range Set	0–0.5	0–100	0–1	0–1	1–2		
	E.P.	0.0364	54.6433	0.7608	0.3251	1.4817		
	RMSE	9.862E-04						
	DDM	$R_s(\Omega)$	$R_{sh}(\Omega)$	I_{ph}(A)	$I_{01}(\mu A)$	a_1	$I_{02}(\mu A)$	a_2
	Range Set	0–0.5	0–100	0–1	0–1	1–2	0–1	1–2
	E.P.	0.0364	53.7804	0.7608	0.0407	1.4495	0.2874	1.4885
	RMSE	9.861E-04						
TLABC	SDM	$R_s(\Omega)$	$R_{sh}(\Omega)$	I_{ph}(A)	$I_0(\mu A)$	a		
	Range Set	0–0.5	0–100	0–1	0–1	1–2		
	E.P.	0.0364	53.7164	0.7608	0.3230	1.4812		
	RMSE	9.8602E-04						
	DDM	$R_s(\Omega)$	$R_{sh}(\Omega)$	I_{ph}(A)	$I_{01}(\mu A)$	a_1	$I_{02}(\mu A)$	a_2
	Range Set	0–0.5	0–100	0–1	0–1	1–2	0–1	1–2
	E.P.	0.0367	54.6680	0.7608	0.4239	1.9075	0.2401	1.4567
	RMSE	9.8414E-04						

Table 8
PV cell parameter identification using WOA variants (57 mm R.T.C. France solar cell).

IWOA	SDM	$R_s(\Omega)$	$R_{sh}(\Omega)$	I_{ph}(A)	$I_0(\mu A)$	a		
	Range Set	0–0.5	0–100	0–1	0–1	1–2		
	E.P.	0.0364	53.7317	0.7608	0.3232	1.4812		
	RMSE	9.8602E-04						
	DDM	$R_s(\Omega)$	$R_{sh}(\Omega)$	I_{ph}(A)	$I_{01}(\mu A)$	a_1	$I_{02}(\mu A)$	a_2
	Range Set	0–0.5	0–100	0–1	0–1	1–2	0–1	1–2
	E.P.	0.0367	55.4082	0.7608	0.6771	2.0000	0.2355	1.4545
	RMSE	9.8255E-04						
CWOA	SDM	$R_s(\Omega)$	$R_{sh}(\Omega)$	I_{ph}(A)	$I_0(\mu A)$	a		
	Range Set	0–0.5	0–100	0–1	0–1	1–2		
	E.P.	0.0364	53.7987	0.7608	0.3239	1.4812		
	RMSE	9.8602E-04						
	DDM	$R_s(\Omega)$	$R_{sh}(\Omega)$	I_{ph}(A)	$I_{01}(\mu A)$	a_1	$I_{02}(\mu A)$	a_2
	Range Set	0–0.5	0–100	0–1	0–1	1–2	0–1	1–2
	E.P.	0.0367	55.2016	0.7608	0.2415	1.4565	0.6000	1.9899
	RMSE	9.8272E-04						

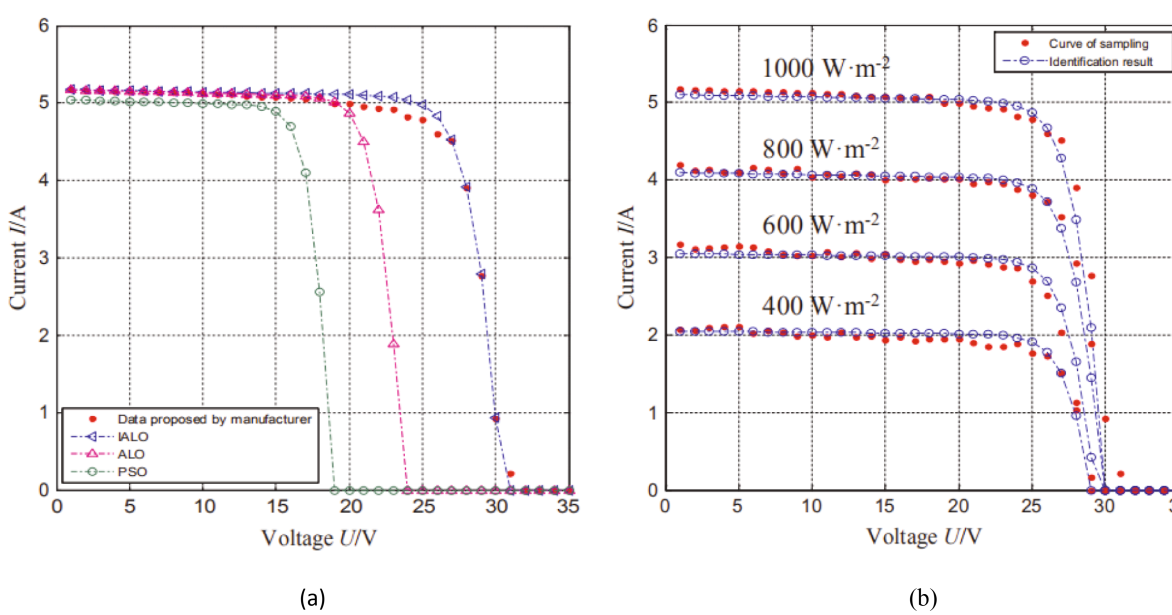

Fig. 2. The output *I-V* curve achieved by (a) different methods; (b) IAIO under different solar irradiation [96].

4.1.9. Bird mating optimization

Bird mating optimization (BMO) algorithm mimics the mating behaviors of birds, in which four distinct searching patterns are utilized in BMO to improve the global optimum searching efficiency [104]. To remedy the drawbacks of original BMO, a simplified BMO (SBMO) has been proposed in [105], which reclassifies the types of the birds into a clearer way based on their fitness value and alleviates the high burden required for parameter assigning.

Meanwhile, the modified rules utilized by SBMO offer an appropriate trade-off between local exploitation and global exploration. At last, Table 11 illustrates the results obtained by BMO for PV cell parameter identification.

Table 9
PV cell parameter identification using BBO-M (57 mm R.T.C. France solar cell).

BBO-M	SDM	$R_s(\Omega)$	$R_{sh}(\Omega)$	$I_{ph}(A)$	$I_0(\mu A)$	a		
	Range Set	0-0.5	0-100	0-1	0-E-06	1-2		
	E.P.	0.0364	53.3623	0.7608	0.3187	1.4798		
	RMSE	9.8634E-04						
	DDM	$R_s(\Omega)$	$R_{sh}(\Omega)$	$I_{ph}(A)$	$I_{01}(\mu A)$	a_1	$I_{02}(\mu A)$	a_2
	Range Set	0–0.5	0–100	0–1	0–E–06	1–2	0–E–06	1–2
	E.P.	0.0366	55.0494	0.7608	0.5912	2	0.2452	1.4580
	RMSE	9.8272E-04						

Table 10
PV cell parameter identification using CS and its variant (57 mm R.T.C. France solar cell).

CS	SDM	$R_s(\Omega)$	$R_{sh}(\Omega)$	$I_{ph}(A)$	$I_0(\mu A)$	a		
	Range Set	0–0.5	0–100	0–1	0–1	1–2		
	E.P.	0.0364	53.7185	0.7608	3.23E-07	1.4812		
	RMSE	0.0010						
BHCS	SDM	$R_s(\Omega)$	$R_{sh}(\Omega)$	$I_{ph}(A)$	$I_0(\mu A)$	a		
	Range Set	0–0.5	0–100	0–1	0–1	1–2		
	E.P.	0.03638	53.7185	0.7608	0.32302	1.4812		
	RMSE	9.8602E-04						
	DDM	$R_s(\Omega)$	$R_{sh}(\Omega)$	$I_{ph}(A)$	$I_{01}(\mu A)$	a_1	$I_{02}(\mu A)$	a_2
	Range Set	0–0.5	0–100	0–1	0–1	1–2	0–1	1–2
	E.P.	0.03674	55.4854	0.7608	0.74935	2.0000	0.2260	1.4510
	RMSE	9.8248E-04						

Table 11
PV cell parameter identification using BMO (57 mm R.T.C. France solar cell).

BMO	SDM	$R_s(\Omega)$	$R_{sh}(\Omega)$	$I_{ph}(A)$	$I_0(\mu A)$	a		
	Range Set	0–0.5	0–100	0–1	0–1	1–2		
	E.P.	0.0364	53.8716	0.7608	0.3248	1.4817		
	RMSE	9.8608E-04						
	DDM	$R_s(\Omega)$	$R_{sh}(\Omega)$	$I_{ph}(A)$	$I_{01}(\mu A)$	a_1	$I_{02}(\mu A)$	a_2
	Range Set	0–0.5	0–100	0–1	0–1	1–2	0–1	1–2
	E.P.	0.0368	55.8081	0.7608	0.2111	1.4453	0.8769	2
	RMSE	9.8262E-04						

4.1.10. Flower pollination algorithm

Flower pollination algorithm (FPA) mainly replicates the pollination process of flowers, in which two pollination methods are employed, i.e., abiotic pollination and biotic pollination [106,107]. Such process can be considered as the optimum searching, as follows [107]:

$$x_i^{t+1} = x_i^t + \gamma L(\lambda)(g_* - x_i^t) \tag{9}$$

where x_i^{t+1} represents the resultant pollen; $L(\lambda)$ means the Lévy flights-based step size; x_i^t denotes the current pollen; γ is a scaling factor; and g_* means the best solution, respectively.

For the sake of improving the convergence speed and exploitation ability, a new hybrid bee pollinator FPA (BPFPA) has been proposed in reference [108], in which simplex method is utilized to generate poor quality solutions to enhance the randomness. Besides, mutation is synthesized into the local search to achieve a wider searching ability. Lastly, the simulated output characteristics of BPFPA for parameter identification are demonstrated in Fig. 3 [108].

4.1.11. Grey wolf optimization

Grey wolf optimization (GWO) algorithm is mainly based on the cooperative hunting behavior of grey wolves [109,110], in which the best, second best and third best solutions in the searching space are called alpha (α), beta (β) and delta (δ), respectively. Meanwhile, the lowest ranking grey wolves are omega (ω) which are always considered as the scapegoats and followers [111].

During the hunting process, the three best solutions will be saved and utilized by the other searching agents (wolves) for position updating. In particular, the final attacking position is determined simultaneously by the positions of α, β, and δ in the searching space. The advantages of such strategy, such as simple structure, high flexibility and strong global exploration ability enable GWO to accurately identify

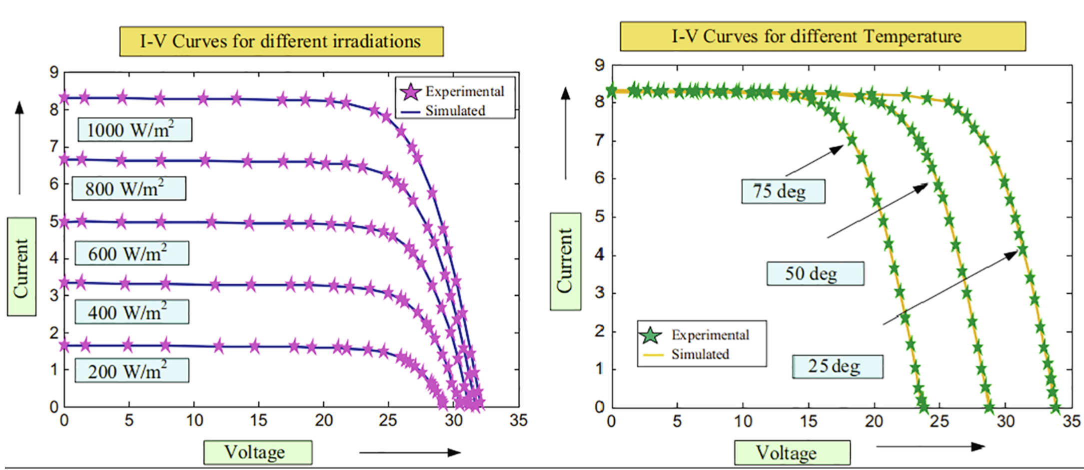

Fig. 3. The simulated output *I-V* curve of BPFPA (KC200GT PV module). (a) different temperature; (b) different irradiation.

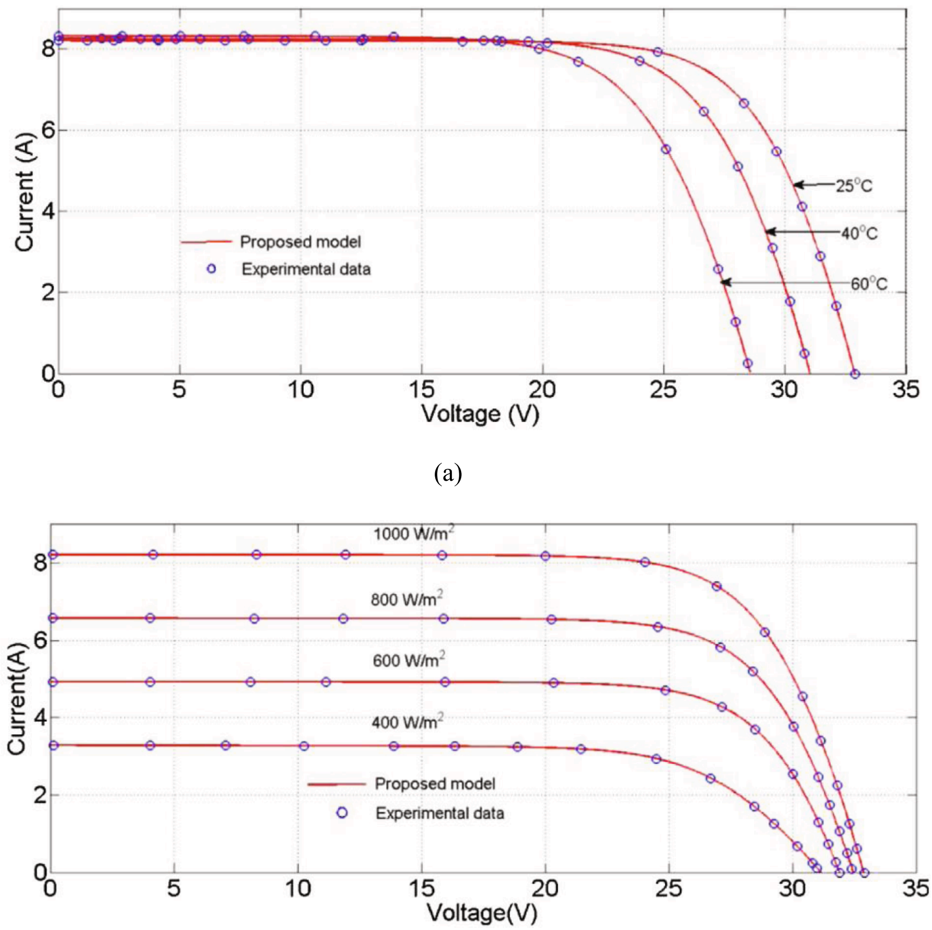

(b)

Fig. 4. The output *I-V* curve of GWO (KC200GT PV module). (a) different temperature; (b) different irradiation [112].

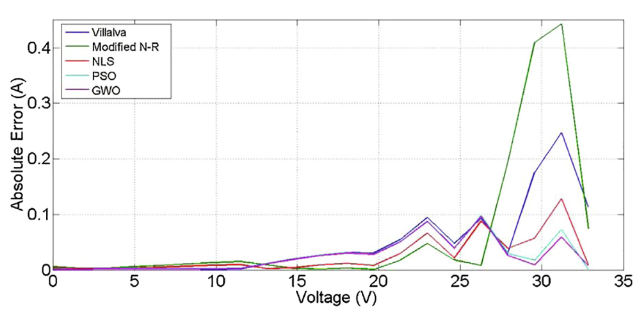

Fig. 5. The comparison of AE obtained by various methods under STC [112].

Table 12
PV cell parameter identification using BFA (SM55 PV cell).

BFA	SDM	$R_s(\Omega)$	$R_{sh}(\Omega)$	I_{ph}(A)	$I_0(\mu A)$	a
	Range Set	0–2	50–500	N.E.	N.E.	1–2
	E.P.	Varies with G &T	Varies with G &T	A.I.	Varies with G &T	A.I.

Table 13
PV cell parameter identification using AIS (SM55 PV cell).

AIS	DDM	$R_s(\Omega)$	$R_{sh}(\Omega)$	I_{ph}(A)	$I_{01}(\mu A)$	a_1	$I_{02}(\mu A)$	a_2
	Range Set	N.S.	N.S.	N.I.	N.S.	N.S.	N.S.	N.S.
	E.P.	0.54741	410.55	N.S.	2.35 E-08	1.2	1.12 E-10	1
	AE	3.41E-05						

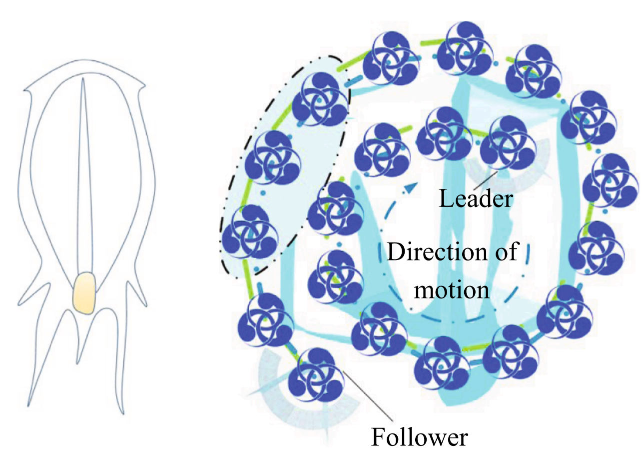

(a) (b)

Fig. 6. (a) Individual salp; (b) salps chain [119].

the parameters under different scenarios [112]. Fig. 4 demonstrates the output *I-V* curve from the parameter identification result using GWO under different weather condition, while the comparison of AE of several approaches is demonstrated in Fig. 5 [112].

4.1.12. Bacterial foraging algorithm

Bacterial foraging algorithm (BFA) replicates the foraging behavior

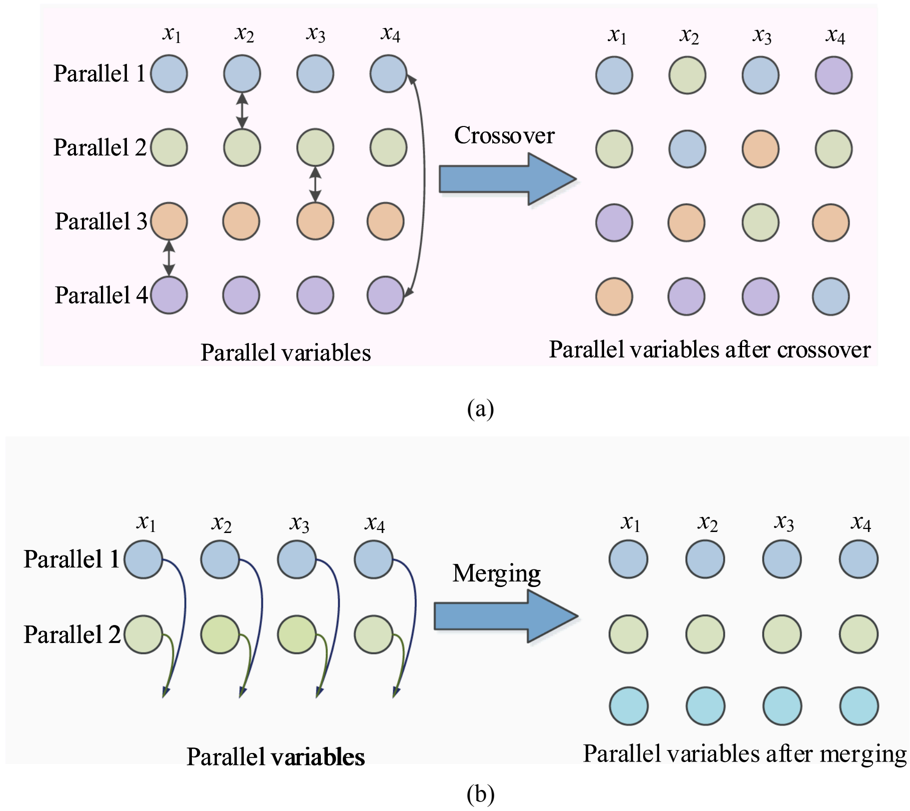

Fig. 7. (a) Crossover operation; (b) Merging operation.

Table 14
PV cell parameter identification using MPCOA (57 mm R.T.C. France solar cell).

MPCOA	SDM	$R_s(\Omega)$	$R_{sh}(\Omega)$	$I_{ph}(A)$	$I_0(\mu A)$	a		
	Range Set	0–0.5	0–100	0–1	0–1	1–2		
	E.P.	0.0364	54.6328	0.7607	0.3366	1.4817		
	RMSE	9.4457E-04						
	DDM	$R_s(\Omega)$	$R_{sh}(\Omega)$	$I_{ph}(A)$	$I_{01}(\mu A)$	a_1	$I_{02}(\mu A)$	a_2
	Range Set	0–0.5	0–100	0–1	0–1	1–2	0–1	1–2
	E.P.	0.0364	54.2531	0.7608	0.3126	1.4784	0.0453	1.7846
	RMSE	9.2163E-04						

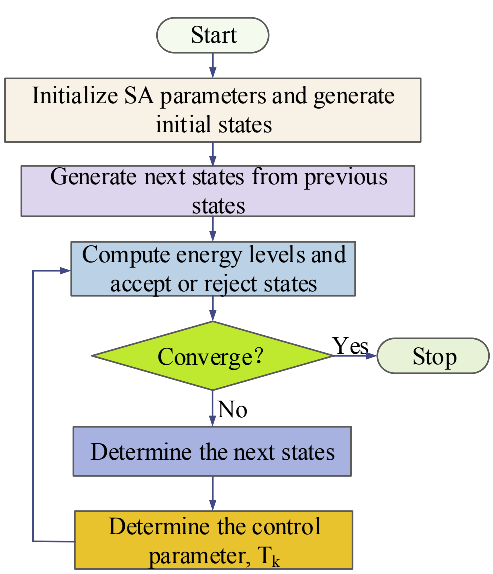

Fig. 8. Flowchart for SA method.

of E-coli bacteria [113]. Particularly, the bacteria with high fitness value will have a chance to spilt into two individuals, thus the population size can be maintained stably [114].

Besides, for the sake of enhancing the population diversity and avoiding being trapped at a local optimum, the bacteria may be eliminated and dispersed when environmental conditions suddenly change [62]. Since BFA is insensitive to the initial values, and the elimination and reproduction phase can effectively enhance the exploitation ability, such strategy has been widely applied on various optimization problem with no derivative information. Lastly, the PV cell parameter identification results based on BFA is demonstrated in Table 12.

4.1.13. Artificial immune system

Artificial immune system (AIS) algorithm is based on the mechanism of human immune system against harmful microorganisms called pathogens [115]. Actually, all produced antibodies share the opportunities to move toward the antigen, while the healthy antibody will be located and added to the memory cells according to the affinity. Particularly, the selection of healthy antibody is mainly based on two factors, i.e., density probability and fitness probability, while the latter one can be described by [116]

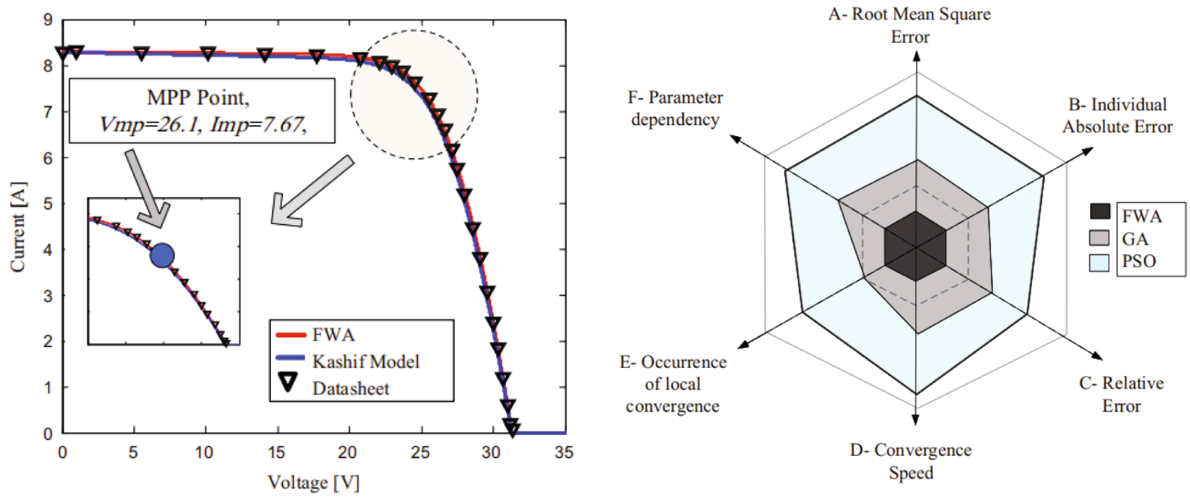

(a) (b)

Fig. 9. (a) The simulated output *I-V* curve of FWA; (b) performance comparison of various methods [63].

Table 15
PV cell parameter identification using WDO (KC200GT PV module).

WDO	SDM	$R_s(\Omega)$	$R_{sh}(\Omega)$	I_{ph}(A)	$I_0(\mu A)$	a		
	Range Set	0.01–0.5	100–1000	N.S	N.S	1–2		
	E.P.	0.1132	747.41	8.1812	0.4423	1.4172		
	RMSE	0.00084						
	DDM	$R_s(\Omega)$	$R_{sh}(\Omega)$	I_{ph}(A)	$I_{01}(\mu A)$	a_1	$I_{02}(\mu A)$	a_2
	Range Set	0.01–0.5	100–1000	N.S	N.S	1–2	N.S	1–2
	E.P.	0.99	784.41	8.1914	4.746×10^{-5}	1.9667	1.632×10^{-6}	1.5370
	RMSE	0.00106						

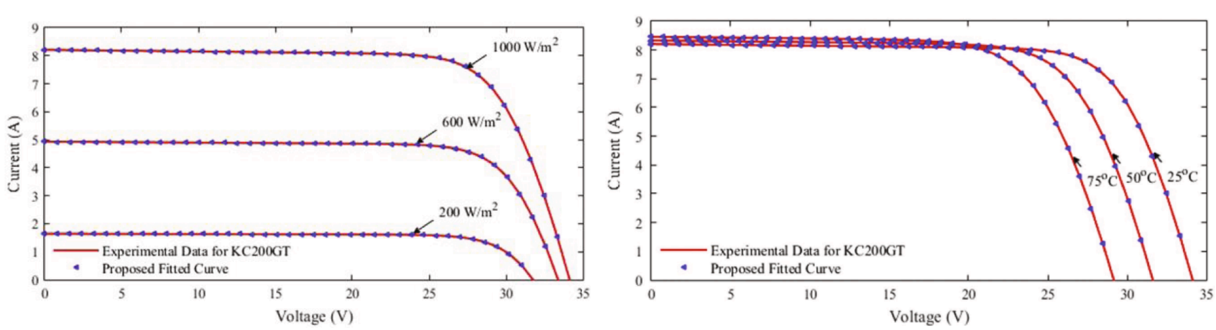

(a) (b)

Fig. 10. The output *I-V* curve of ER-WCA (KC200GT PV module): (a) different irradiation; (b) different temperature [65].

Table 16
PV cell parameter identification using LCOA and its variant (57 mm R.T.C. France solar cell).

LCOA	SDM	$R_s(\Omega)$	$R_{sh}(\Omega)$	I_{ph}(A)	$I_0(\mu A)$	a		
	Range Set	0–0.5	0–100	0–1	0–1	1–2		
	E.P.	0.0364	53.9024	0.7608	0.3233	1.4812		
	RMSE	9.8609E-04						
	DDM	$R_s(\Omega)$	$R_{sh}(\Omega)$	I_{ph}(A)	$I_{01}(\mu A)$	a_1	$I_{02}(\mu A)$	a_2
	Range Set	0–0.5	0–100	0–1	0–1	1–2	0–1	1–2
	E.P.	0.3667	54.6314	0.7608	0.2661	1.4621	0.3802	1.9938
	RMSE	9.8423E-03						
ILCOA	SDM	$R_s(\Omega)$	$R_{sh}(\Omega)$	I_{ph}(A)	$I_0(\mu A)$	a		
	Range Set	0–0.5	0–100	0–1	0–1	1–2		
	E.P.	0.0364	53.7187	0.7608	0.3230	1.4811		
	RMSE	9.8602E-04						
	DDM	$R_s(\Omega)$	$R_{sh}(\Omega)$	I_{ph}(A)	$I_{01}(\mu A)$	a_1	$I_{02}(\mu A)$	a_2
	Range Set	0–0.5	0–100	0–1	0–1	1–2	0–1	1–2
	E.P.	0.0367	55.5320	0.7608	0.2260	1.451	0.7492	2
	RMSE	9.8257E-04						

Table 17
The pseudo code of new harmony improvisation.

```
for j = 1:d
  if r1≥HMCR
    xnew (j) = l (j) + r2×(u(j)−l(j));
  else
    n = the index of a harmony from HM
    xnew (j) = HM (n,j);
    if r3<PAR
      xnew (j) = xnew (j) + (r4-r5)×b×|u(j)−l(j)|;
    end
  end
end
```

$$p_{\mathrm{f},i} = \frac{f(x_i)}{\sum_{j=1}^{s} f(x_i)} \tag{10}$$

where $p_{\mathrm{f},i}$ represents the fitness probability of the ith antibody; $f(x_i)$ denotes the fitness value of the ith antibody; and S represents the number of all antibodies, respectively.

Besides, crossover and mutation can effectively improve the diversity of antibodies, which can significantly avoid premature convergence. Finally, the simulated results obtained by AIS is tabulated in Table 13.

4.1.14. Salp swarm algorithm

Salp swarm algorithm (SSA) is a novel biology-based algorithm inspired by the unique collaborative chains foraging mechanism of salps in oceans [117,118]. This salp swarm pattern called salp chain can effectively mitigate the inertia to the local optimum, which consists of two groups, i.e., leader and followers, as shown Fig. 6 [119].

In order to verify the practical performance of SSA, TITAN-12-50 panel is utilized for PV cell parameter identification. Particularly, the simulated results can verify that SSA has the superiorities, such as high convergence speed and strong ability to escape local optimum under stagnation scenario. Hence, such strategy can be considered as a powerful and reliable tool to solve identification problem of PV cells.

4.2. Physics-based algorithms

4.2.1. Particle swarm optimization

PSO is a parallel global random searching strategy derived from the foraging behavior of birds [120], in which the particle swarm follows the global and individual optimal directions to update its velocity and position [121,122].

Since PSO has shown excellent flexibility and practicality in solving various complex optimization problems [123], many improved variants, e.g., flexible PSO (FPSO) [124], guaranteed convergence PSO (GCPSO) [125], parallel PSO (PPSO) [126], time varying acceleration coefficients PSO (TVACPSO) [127], enhanced leader PSO (ELPSO) [128] are proposed to further enhance the overall performance and have been applied on parameter identification. For instance, a scale factor is introduced in GCPSO to modify the velocity equation of the global best particle, which can effectively avoid premature convergence, as follows [125]:

$$v_{\psi,i}(t+1) = x_{\psi,i} + G_{\mathrm{b}} + \chi v_{\psi,i}(t+1) + \rho(t)(1-2r_1) \tag{11}$$

where ψ represents the global best particle index; G_{b} denotes the best position of the particles; r_1 represents a random number between 0 and 1; $x_{\psi,i}$ means the current position of the ith particle; $\rho(t)$ represents the scale factor; $v_{\psi,i}(t+1)$ and $v_{\psi,i}$ denote the updated velocity and the current velocity of the ith particle, respectively.

Moreover, TVACPSO can effectively enhance the accuracy through setting appropriate trade-off between local exploitation and global exploration. Besides, the five-staged successive mutation strategy utilized in ELPSO can efficiently improve the global exploration ability and avoid premature convergence.

4.2.2. Mutative scale parallel chaos optimization algorithm

Compared with the conventional parallel chaos optimization algorithm (PCOA) [129], two operations, i.e., crossover operation and merging operation between two randomly selected parallel variables are introduced in MPCOA to expand the searching space, which are demonstrated in Fig. 7 [130].

When the chaotic map is mapped onto the variance range of decision variable, the expression can be given by

$$X_{ij}(k) = L_i + \gamma_{ij}(k)(U_i - L_i) \tag{12}$$

where $\gamma_{ij}(k)$ represents the chaotic map; $X_{ij}(k)$denotes the decision variable; while L_i and U_i are lower and upper limits, respectively.

At last, Table 14 represents the results obtained by MPCOA for PV cell parameter identification.

Table 18
PV cell parameter identification using TLBO and its variants (57 mm R.T.C. France solar cell).

TLBO	SDM	$R_s(\Omega)$	$R_{sh}(\Omega)$	$I_{ph}(A)$	$I_0(\mu A)$	a		
	Range Set	0–0.5	0–100	0–1	0–1	1–2		
	E.P.	0.0364	53.7187	0.76074	0.3238	1.4852		
	RMSE	9.8845E-04						
	DDM	$R_s(\Omega)$	$R_{sh}(\Omega)$	$I_{ph}(A)$	$I_{01}(\mu A)$	a_1	$I_{02}(\mu A)$	a_2
	Range Set	0–0.5	0–100	0–1	0–1	1–2	0–1	1–2
	E.P.	0.0365	55.8459	0.7607	0.2029	1.9981	0.2995	1.4749
	RMSE	9.9507E-04						
STLBO	SDM	$R_s(\Omega)$	$R_{sh}(\Omega)$	$I_{ph}(A)$	$I_0(\mu A)$	a		
	Range Set	0–0.5	0–100	0–1	0–1	1–2		
	E.P.	0.0364	53.7187	0.7608	0.3230	1.4811		
	RMSE	9.8602E-04						
	DDM	$R_s(\Omega)$	$R_{sh}(\Omega)$	$I_{ph}(A)$	$I_{01}(\mu A)$	a_1	$I_{02}(\mu A)$	a_2
	Range Set	0–0.5	0–100	0–1	0–1	1–2	0–1	1–2
	E.P.	0.0368	55.4920	0.7608	0.2257	1.4508	0.7522	2
	RMSE	9.8272E-04						
GOTLBO	SDM	$R_s(\Omega)$	$R_{sh}(\Omega)$	$I_{ph}(A)$	$I_0(\mu A)$	a		
	Range Set	0–0.5	0–100	0–1	0–1	1–2		
	E.P.	0.0363	54.1154	0.7608	0.3316	1.4838		
	RMSE	9.8744E-04						
	DDM	$R_s(\Omega)$	$R_{sh}(\Omega)$	$I_{ph}(A)$	$I_{01}(\mu A)$	a_1	$I_{02}(\mu A)$	a_2
	Range Set	0–0.5	0–100	0–1	0–1	1–2	0–1	1–2
	E.P.	0.0368	56.0753	0.7608	0.8002	1.9999	0.2205	1.4489
	RMSE	9.8318E-04						

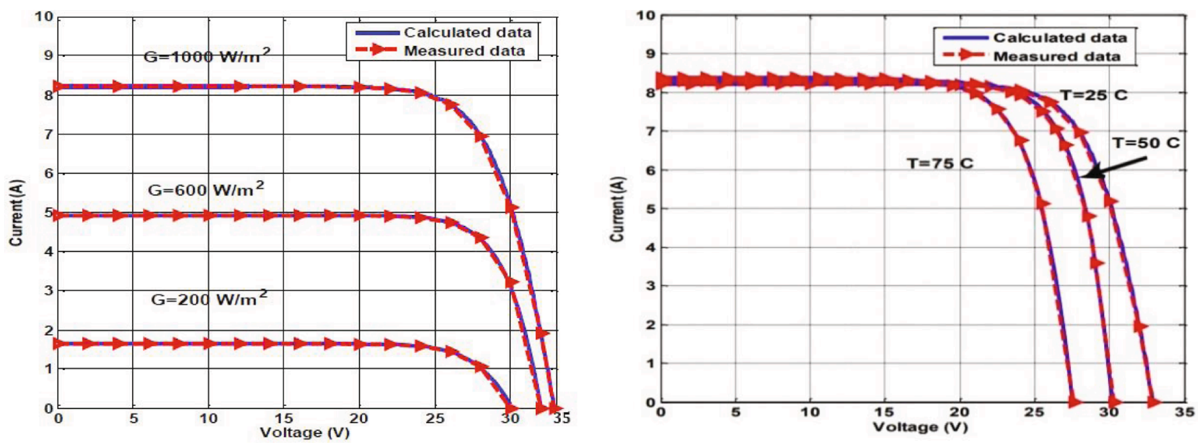

(a) (b)

Fig. 11. The output *I-V* curve of ICA (KC200GT PV module): (a)different irradiation; (b) different temperature [70].

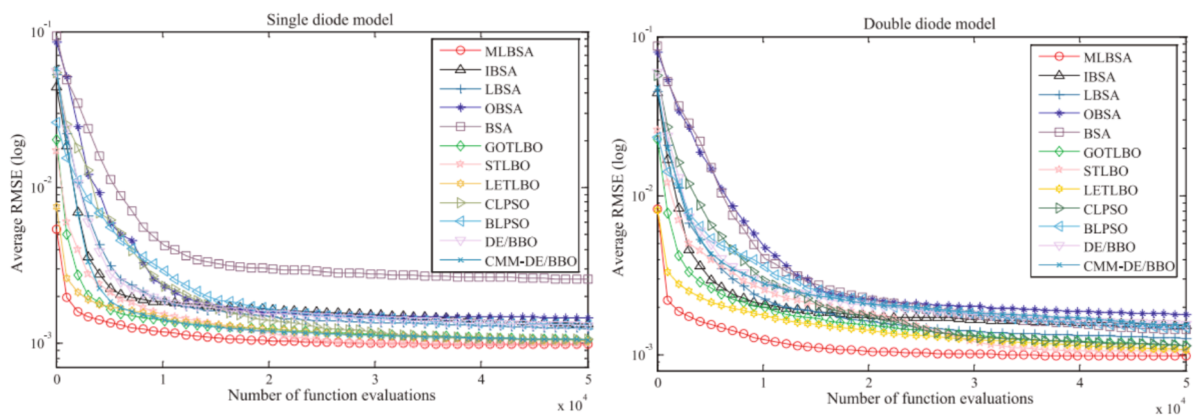

(a) (b)

Fig. 12. The average RMSE of various methods (R.T.C. France solar cell): (a) SDM; (b) DDM [142].

Table 19
PV cell parameter identification using PS (57 mm R.T.C. France solar cell).

PS	SDM	$R_s(\Omega)$	$R_{sh}(\Omega)$	I_{ph}(A)	$I_0(\mu A)$	a		
	Range Set	N.S	N.S	N.S	N.S	N.S		
	E.P.	0.0313	64.1026	0.7617	0.9980	1.6		
	RMSE	0.2863						
	DDM	$R_s(\Omega)$	$R_{sh}(\Omega)$	I_{ph}(A)	$I_{01}(\mu A)$	a_1	$I_{02}(\mu A)$	a_2
	Range Set	N.S	N.S	N.S	N.S	N.S	N.S	N.S
	E.P.	0.032	81.3008	0.7602	0.9889	1.0.6	0.0001	1.192

4.2.3. Simulated annealing algorithm

Simulated annealing (SA) algorithm is inspired by the physical gradual cooling process called annealing, while its flowchart is demonstrated in Fig. 8, as follows [131]:

The hybrid method (LM + SA) combines Levenberg-Marquardt (LM) method with SA has already been applied on parameter identification [132], such strategy is mainly depended on the proper setting of damping factor [133] of LM. From the results of SA application on PV cell parameter identification, it can be found that changing the irradiation levels will not basically influence the identification results. Meanwhile, SA based damping factor control can effectively improve the global searching ability of LM method, which can help seek a global optimum.

4.2.4. Fireworks algorithm

Fireworks algorithm (FWA) is based on the fireworks explosion mechanism in the air. The stochastic explosion of fireworks can be regarded as a continual search around a particular point in the local space, in which the new sparks generated by the fireworks can be regarded as potential solutions to the optimization [63]. Basically, the spark evaluation of fireworks under the given objective function can be given by

$$S_i = m\bullet\frac{y_{\max} - f(x_i) + \xi}{\sum_{i=1}^{n}(y_{\max} - f(x_i) + \xi)} \tag{13}$$

where S_i represents the spark evaluation of the ith firework; m is the control parameter responsible for the number of sparks generated; $f(x_i)$ denotes the objective function of the ith firework; $y_{\max}$ represents the maximum objective function $f_{\max}(x_i)$; and ξ denotes an extreme small positive number, respectively.

Since Gaussian mutation operator is combined with FWA, such strategy can significantly enhance the local searching ability and create randomness. Besides, FWA can effectively balance local exploitation and global exploration to avoid premature convergence. The simulated *I-V* output curve of FWA and the performance comparison of various methods under KC200GT PV module are demonstrated in Fig. 9 [63].

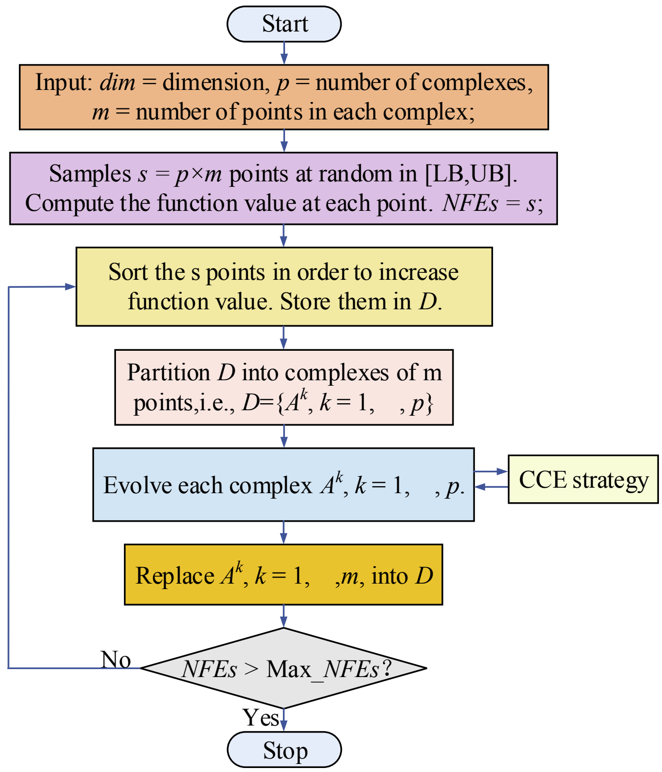

Fig. 13. Flowchart for SCE.

4.2.5. Wind driven optimization

Wind driven optimization (WDO) algorithm mainly replicates the motion of microscopic air parcels in a multidimensional space [134]. In particular, the velocity and position of each air parcel need to be updated continuously to explore new searching space, as follows [135]:

$$\vec{u}_{\text{new}} = (1-\alpha)\vec{u}_{\text{cur}} - gx_{\text{cur}} + \left(\left|1-\frac{1}{i}\right|\bullet(x_{\text{opt}}-x_{\text{cur}})RT\right) + (\frac{c\bullet\vec{u}_{\text{od}}}{i}) \tag{14}$$

where $\vec{u}_{\text{new}}$ represents the velocity of next iteration; α denotes the frictional coefficient $\vec{u}_{\text{cur}}$ means the velocity of current iteration; x_{cur} represents the current position of the air parcel; i denotes the rank of the air parcel; x_{opt} means the optimal position of air parcel; $c = -2RT$; and $\vec{u}_{\text{od}}$ is equal to Coriolis force $\vec{F_c}$, respectively.

Since WDO is easy to implement and only needs few adjustable parameters, it has the merits of strong global searching ability, fast convergence, and strong robustness. The results obtained by WDO are demonstrated in Table 15.

4.2.6. Evaporation rate based water cycle algorithm

Evaporation rate based water cycle algorithm (ER-WCA) is an improved version of water cycle algorithm (WCA) [136] mimicking the water cycle process in nature. Initially, a part of streams are generated and chosen as sea and rivers according to their fitness value. Meanwhile, according to the intensity of flow, the streams may have a chance to flow into the rivers or sea. On the other hand, the best solution (sea) also owns the right to control and owns more streams [65].

Besides, the evaporation process is introduced to avoid premature convergence, while the raining process can form new streams in various directions, as follows:

$$\vec{X}_{\text{st}}^{\text{new}}(t+1) = \vec{L}_{\text{b}} + r\bullet(\vec{U}_{\text{b}} - \vec{L}_{\text{b}}) \tag{15}$$

where $\vec{X}_{\text{st}}^{\text{new}}$ represents the new generated stream; r means a random number uniformly distributed between 0 and 1; $\vec{U}_{\text{b}}$ and $\vec{L}_{\text{b}}$ mean the lower and upper bounds, respectively.

Lastly, the output *I-V* curves of ER-WCA for PV cell parameter identification under various weather scenarios are demonstrated in Fig. 10 [65].

4.2.7. Lozi map-based chaotic optimization algorithm

Since chaos systems have been widely combined with random optimization algorithms and has achieved promising results, Lozi map-based chaotic optimization algorithm (LCOA) has been utilized for solving various optimizations. However, as the distribution of density in Lozi map is uneven, which usually leads to a large number of relatively weak or worthless searches, especially for chaotic global search. Hence, an improved LCOA (ILCOA) [137] is proposed to remedy the drawbacks, such as unstable results and inadequate global searching ability. Particularly, semi-exponentially step size (SESS) is adopted in ILCOA, which focuses on small λ and strengthens the exploitation ability for higher quality optimums.

Lastly, for the sake of testifying the practical performance of two strategies, both two approaches have been utilized in PV cells parameter identification, while the results are tabulated in Table 16.

4.3. Sociology-based algorithms

4.3.1. Harmony search algorithm

Harmony search (HS) optimization strategy originally replicates the improvisation process of musicians, in which each solution called harmony is specified by a vector [138]. After each iteration, the harmony vectors are stored in the harmony memory (HM) while a better harmony will replace the worst harmony stored in HM to ensure high-quality harmonies. Particularly, the pseudo code of new harmony improvisation is provided in Table 17 [64].

Besides, an improved variant called grouping-based global harmony search (GGHS) [64] can effectively exploit the potential optimum based on the consideration that there may exist useful information in the worst harmonies. Besides, an elite strategy is introduced in innovative global

Table 20
PV cell parameter identification using SCE variants (57 mm R.T.C. France solar cell).

ISCE	SDM	$R_s(\Omega)$	$R_{sh}(\Omega)$	$I_{ph}(A)$	$I_0(\mu A)$	a		
	Range Set	0–0.5	0–100	0–1	0–1	1–2		
	E.P.	0.0364	53.7185	0.76078	0.3230	1.4812		
	RMSE	9.8602E-04						
	DDM	$R_s(\Omega)$	$R_{sh}(\Omega)$	$I_{ph}(A)$	$I_{01}(\mu A)$	a_1	$I_{02}(\mu A)$	a_2
	Range Set	0–0.5	0–100	0–1	0–1	1–2	0–1	1–2
	E.P.	0.0367	55.4854	0.7608	0.2260	1.4510	0.7494	2
	RMSE	9.8248E-04						
ESCE-OBL	DDM	$R_s(\Omega)$	$R_{sh}(\Omega)$	$I_{ph}(A)$	$I_{01}(\mu A)$	a_1	$I_{02}(\mu A)$	a_2
	Range Set	0–0.5	0–100	0–1	0–1	1–2	0–1	1–2
	E.P.	0.0367	55.4854	0.7608	0.2260	1.4410	0.7494	2
	RMSE	9.8248E-04						

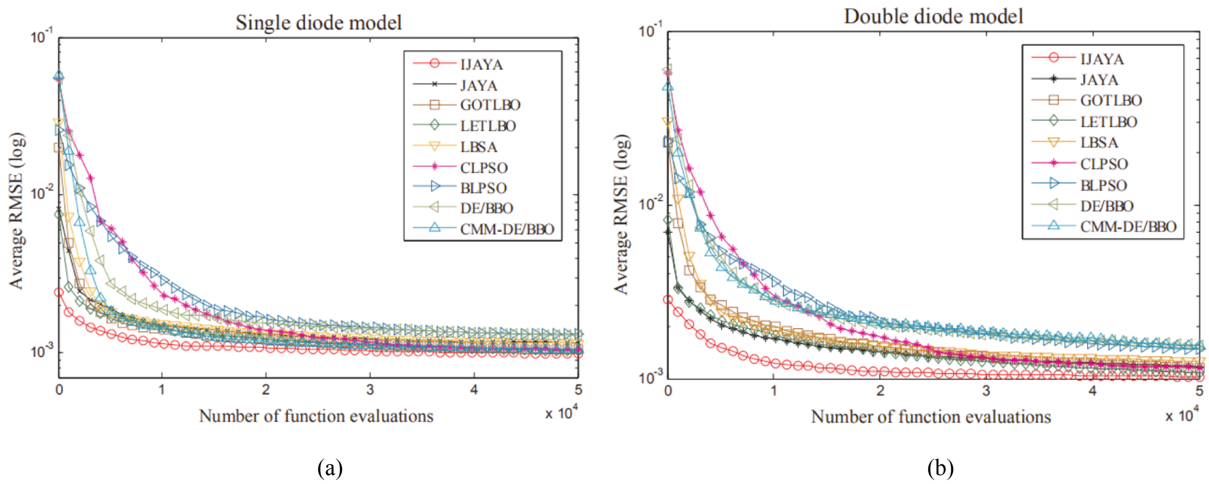

Fig. 14. The average RMSE of various methods (R.T.C. France solar cell): (a) SDM; (b) DDM [148].

harmony search (IGHS) [64]. In general, these variants can effectively remedy the drawbacks of original HS and are also applied on PV parameter identification, in which the accuracy of IGHS is the highest.

4.3.2. Teaching learning based optimization

Teaching learning based optimization (TLBO) algorithm mainly mimics the teaching-learning behavior in the classroom, which are mainly composed of two phases, i.e., teaching and learning [139].

In addition, an improved and simplified TLBO (STLBO) algorithm has been proposed in reference [140], in which an elite strategy and local searching are adopted to effectively improve the global searching ability. Besides, STLBO remains the merits of simple structure and easy implementation. Moreover, a generalized oppositional TLBO (GOTLBO) [141] is proposed to enhance the convergence and simplify the structure, in which the initialization step and opposition-based generation jumping strategy are introduced. Lastly, the results acquired by TLBO and its variants for parameter identification are illustrated in Table 18.

4.3.3. Imperialist competitive algorithm

Imperialist competitive algorithm (ICA) is mainly based on the mechanism of imperialistic competition, which divides the initial countries into two groups, i.e., imperialist countries which possess the best fitness function value and colonies which follow the imperialists. Particularly, the normalized power of each imperialist country can be described by [70]

$$p_i = \frac{|C_i|}{|\sum_{k=1}^{N_{\mathrm{imp}}} C_k|} \tag{16}$$

where N_{imp} represents the number of imperialist countries; p_i denotes the normalized power of the ith imperialist; and C_i denotes the cost of the ith imperialist country, respectively.

The most powerful empire in the end of iterations can be treated as the optimal solution. Compared with GA and PSO, ICA has a higher convergence speed and accuracy, and stronger convergence stability, especially for low dimensional optimizations. The output *I-V* curve of ICA under various environmental scenarios are demonstrated in Fig. 11 [70].

4.3.4. Multiple learning backtracking search algorithm

The main structure of multiple learning backtracking search algorithm (MLBSA) is based on backtracking search algorithm (BSA). All the individuals in MLBSA are classified into two groups, i.e., (a) individuals utilize the information of current and the historical population, and (b) individuals learn from the best individual of the current population [142]. Such multi-learning strategy can better balance the local exploitation and global exploration, as follows:

$$V_{i,j} = \begin{cases} P_{i,j} + F\cdot[(\mathrm{old}P_{i,j} - P_{i,j}) + (P_{h,j} - P_{i,j})], & \text{if } \left(a < \frac{b}{a},\ b \in U(0,1)\right) \\ P_{i,j} + r\cdot(P_{\mathrm{best},j} - P_{i,j}), & \text{otherwise} \end{cases} \tag{17}$$

where $V_{i,j}$ denotes the value of the jth variable for the ith trial individual; F represents the scale factor that regulates the amplitude of the searching direction matrix; $P_{i,j}$ means the value of the jth variable for the individual i of current population; $P_{h,j}$ denotes the value of the jth variable for the individual h of current population; r, a and b represent three random numbers uniformly distributed between 0 and 1; and $P_{\mathrm{best},j}$ means the value of the jth variable for the current best individual, respectively.

Lastly, the comparison of average RMSE of various methods under SDM and DDM are demonstrated in Fig. 12 [142].

4.4. Mathematics-based algorithms

4.4.1. Pattern search algorithm

Pattern search (PS) is a derivative-free algorithm which merely requires to evaluate the objective function towards its search for optimization [143,144]. In particular, approximations of the objective function are not needed in PS since it can use its own historical search to forecast the direction of new search. Besides, a new objective function is adopted in PS to lead itself to the optimal estimated parameter values [145]. Hence, it can effectively alleviate system modelling from the conventional oversimplifying assumptions. Table 19 represents the results obtained by PS for PV cell parameter identification.

4.4.2. Shuffled complex evolution

Shuffled complex evolution (SCE) algorithm is mainly composed of three phases, i.e., population, complex and simplex [61], in which the utilization of controlled random search and competitive complex evolution (CCE) can efficiently improve its global optimization ability. In particular, the flowchart of SCE is demonstrated in Fig. 13 [146].

However, there are still some shortcomings in SCE, thus an improved shuffled complex evolution (ISCE) is developed in [146] to enhance the convergence speed and better balance the local exploitation and global exploration, in which an improved CCE strategy is utilized.

Besides, in work [147], a new improved shuffled complex evolution algorithm enhanced by the opposition-based learning strategy (ESCE-OBL) is proposed, in which OBL method is utilized to noticeably enhance the quality of initial solutions while ESCE strategy can effectively accelerate the convergence. In particular, the results acquired by SCE

Table 21
Summary of meta-heuristic algorithms applied on PV cell/module parameter identification.

Classification	Algorithms	Year	SDM	DDM	PV cell/module	Used data	Advantages	Disadvantages
Biology-based	GA [69]	2001	✓		57 mm diameter R.T.C. France solar cell	Experimental *I-V* data	a) always can find promising region of search space; b) acceptable accuracy.	a) easily converge to local optimum; b) lack of local searching ability.
	DE [35]	2011	✓		SM55 PV cell	Manufacturer's experimental data	a) desirable accuracy under various weather conditions; b) excellent exploration ability.	a) sensitive parameter setting; b) weak practicality of mutation strategy; c) lack of exploitation ability.
	ABSO [83]	2013	✓	✓	57 mm diameter R.T.C. France solar cell	*I-V* characteristics resulted from the experimental data obtained from the real system	a) satisfactory flexibility; b) proper balance between global exploration and local exploitation; c) high effectiveness.	a) the solution could be a high-quality local optimum rather than global optimum; b) stagnation during the iteration.
	ABC [85]	2014	✓	✓	57 mm diameter R.T.C. France solar cell	Experimental data	a) strong robustness and high accuracy; b) no sensitivity to noisy conditions; c) low probability to fall into local optimum; d) simple calculation.	a) long searching time; b) sensitive parameter setting; c) premature convergence.
	WOA [94]	2017	✓	✓	KC200GT PV module	Experimental outcomes of KC200GT PV module and other optimisation methods	a) simple structure; b) low computational burden and high convergence peed; d) good local exploitation ability.	a) lack of global exploration ability; b) easily trapped at local optimum during the last stage of the algorithm; c) premature convergence.
	IAIO [96]	2017	✓		N.S.	Data from the manufacturer	a) high convergence rate; b) avoid premature convergence; c) high accuracy.	N.S.
	BBO [99]	2014	✓	✓	57 mm diameter R.T.C. France solar cell	Experimental data	a) high quality of solution; b) fast convergence speed.	a) lack of exploitation ability; b) premature convergence.
	CS [102]	2013	✓		57 mm diameter R.T.C. France solar cell	Experimental data	a) high accuracy; b) high global exploration ability.	a) slow convergence.
	BMO [104]	2013	✓	✓	57 mm diameter R.T.C. France solar cell	*I-V* characteristics resulted from the experimental data	a) effectively avoid premature convergence; b) high accuracy.	a) complex parameter setting; b) complex classification of birds.
	FPA [107]	2015	✓	✓	KC200GT PV module	Experimental data from manufacturer's datasheet	a) high convergence speed; b) excellent global searching ability; c) high accuracy.	a) lack to create randomness; b) poor solution quality.
	GWO [112]	2019	✓		KC200GT PV module	Experimental data under different weather conditions	a) strong robustness under various weather conditions; b) strong ability to avoid local optimum; c) high accuracy and flexibility.	a) convergence speed will slow down in the later period.
	BFA [62]	2013	✓		SM55 PV cell	Experimental data with *I-V* curves	a) high quality and consistency of solutions; b) high computational efficiency; c) high accuracy.	a) low convergence speed.
	AIS [116]	2015		✓	SM55 PV cell	Experimental values of other meta-heuristic algorithms	a) high convergence speed; b) high quality solutions.	N.S.
	SSA [119]	2019		✓	TITAN-12–50 panel	Experimental data	a) high convergence speed; b) stable balance between local exploitation and global exploration. c) strong ability to escape local optimum.	N.S.

(*continued on next page*)

Table 21 (*continued*)

Classification	Algorithms	Year	SDM	DDM	PV cell/module	Used data	Advantages	Disadvantages
Physics-based	PSO [121]	2009	✓	✓	N.S.	Synthetic and experimental current–voltage data	a) high computation efficiency; b) easy implementation; b) strong robustness to control variables.	a) easy to trap at local optimum; b) premature convergence.
	MPCOA [130]	2014	✓	✓	57 mm diameter R.T.C. France solar cell	Real measured *V-I* data	a) good balance between global exploration and local exploitation; b) good accuracy.	N.S.
	SA [131]	2012	✓	✓	57 mm diameter R.T.C. France solar cell	Real measured *I-V* data	a) strong robustness; b) easy implementation.	a)sensitive to initial values; b) low convergence rate.
	FWA [63]	2016		✓	KC200GT PV module	*I-V* datasheet	a) proper balance between exploration and exploitation; b) computational complexity; c) fast convergence.	a) premature convergence; b) lack of high accuracy.
	WDO [135]	2017	✓	✓	KC200GT PV module	Experimental data	a) high accuracy; b) fast convergence; c) high global searching ability.	a) sensitive parameter setting.
	ER-WCA [65]	2017	✓	✓	KC200GT PV module	Experimental data	a) high suitability and effectiveness under various weather conditions; b) good balance between global exploration and local exploitation; c) fast convergence.	a) medium–low solution quality.
	LCOA [137]	2019	✓	✓	57 mm diameter R.T.C. France solar cell	Standard data set for 57 mm diameter R.T.C. France solar cell	a) high convergence rate; b) high accuracy.	a) lack of ability to escape from the local minima; b) lack of stability and robustness.
Sociology-based	HS [64]	2012	✓	✓	57 mm diameter R.T.C. France solar cell	*I-V* characteristic based on experimental data	a) simple concept; b) easy implementation; c) high effectiveness.	a) lack of search capability; b) premature convergence.
	TLBO [139]	2014	✓	✓	57 mm diameter R.T.C. France solar cell	Experimentally measured *I-V* characteristic	a) simple and easy implementation; b) few control variables required; c) high convergence speed.	a) high evaluation cost; b) medium–low quality of solutions.
	ICA [70]	2017	✓	✓	KC200GT PV module	Experimental data and other reported meta-heuristic optimization algorithms	a) high computational efficiency; b) high accuracy.	a) easy to trap at local optimum; b) low convergence speed.
	MLBSA [142]	2018	✓	✓	57 mm diameter R.T.C. France solar cell	Experimental data set	a) proper balance between global exploration and local exploitation; b) high accuracy and reliability; c) low computation burden.	N.S.
Mathematics-based	PS [143]	2011	✓	✓	57 mm diameter R.T.C. France solar cell	Manufacturer datasheet values	a) high robustness efficiency; b) high flexibility.	N.S.
	ISCE [146]	2018	✓	✓	57 mm diameter R.T.C. France solar cell	Standard measured *I-V* data	a) high solution quality; b) strong global searching ability; c) high convergence speed and strong robustness.	a) lack of test and analysis under different operating conditions.
	JAYA [148]	2017	✓	✓	57 mm diameter R.T.C. France solar cell	Experimental data	a) low computation time and implementation complexity; b) simple optimization process; c) high convergence speed and strong robustness.	a) easy to trap at local optimum; b) poor quality of final solution.

Table 22
Comparison of different MPPT meta-heuristic algorithms.

Meta-heuristic algorithms	Year	Complexity	Tracking speed (s)	Efficiency (%)	Converter type	Applications	Exp-Val
Modified GA	2014	Medium	0.83	97 [154]	Buck-Boost	S.A.	Yes
DynNp-DE	2014	Medium	0.95	99.45 [155]	Boost	S.A.	No
SA	2015	High	N.S.	92.17 [156]	Boost	S.A. / G.C.	Yes
Hybrid GWO and P&O	2016	Medium	0.015	100 [157]	Boost	S.A.	Yes
WOA	2016	Medium	1.05	97.99 [158]	Boost	S.A.	Yes
Generalized PS	2016	Medium	N.P.	97.66 [159]	Boost	S.A.	No
WODE	2017	High	1.23	99.10 [160]	N.P.	N.P.	No
Enhanced GWO	2017	High	N.P.	99.93 [161]	Boost	S.A.	No
Leader-PSO	2017	Low	0.35	99.99 [162]	Boost	S.A.	Yes
MPV-PSO	2017	Medium	0.38	99.95 [163]	Boost	S.A.	Yes
Improved PS	2017	Medium	N.P.	97.50 [164]	Boost	S.A.	No
MGA-FA	2018	Medium	0.036	99.26 [165]	Buck	S.A.	Yes
Modified FPA	2018	Medium	0.35	99.90 [166]	Boost	S.A.	Yes
Improved DE	2018	Medium	1.0	99 [167]	SEPIC	S.A.	Yes
WDO	2019	Low	0.088	99.95 [168]	Boost	S.A.	Yes

*Exp-Val: Experimental Validation; S.A.: Stand alone; G.C.: Grid connected; Single-ended primary-inductor converter: SEPIC.

variants for parameter identification are demonstrated in Table 20.

4.4.3. JAYA algorithm

JAYA algorithm only needs two parameters when solving various constrained and unconstrained optimizations, i.e., population size and generation numbers. Furthermore, in order to remedy the disadvantages of JAYA algorithm, e.g., insufficient population diversity, weak global exploration ability, and poor quality of final solution, an improved JAYA (IJAYA) algorithm is proposed [148]. Moreover, a performance-guided JAYA (PGJAYA) algorithm [149] is designed to balance the local exploitation and global exploration more efficiently. In addition, a novel elite opposition-based JAYA (EO-JAYA) algorithm [150] is reported to improve the population diversity.

At last, the comparison of average RMSE of various methods under SDM and DDM are demonstrated in Fig. 14 [148].

In general, based on the simulation performance of PV cell parameter identification under various algorithms, one can readily observe that the accuracy of DDM is slightly higher than SDM measured by evaluation criteria, such as RMSE and MAE. However, since SDM has the superiorities of simple structure and low complexity, upon which it has been widely utilized in the PV systems which require fast *I-V* characteristic responses. Besides, SDM is often applied based on the assumption that the recombination loss in the depletion region can be ignored [54]. Meanwhile, DDM is preferable for the applications which require to replicate precise *I-V* characteristics, especially under low solar irradiation level and varying environmental conditions, e.g., STC. Lastly, TDM has the highest accuracy and complexity, such that it always utilized to describe complicated physical behaviour of larger scale industrial PV systems.

Besides, it is noteworthy that different models cater for various PV devices from the simulation performance, such as both SDM and DDM can always output the best simulation results based on poly-crystalline R.T.C. France solar cell compared with other solar devices, such as mono-crystalline SM55 PV cell, and poly-crystalline KC200GT PV module [70,93,102,135]. Meanwhile, both SDM and DDM can better fit mono-crystalline SM55 PV cell than poly-crystalline KC200GT PV module [35,63,116].

5. Discussions

5.1. Overall summary

Various meta-heuristic algorithms which have been applied on PV cell parameters identification are introduced in the last part, while it is difficult to acquire an overall and comprehensive comparison. Hence, Table 21 aims to discuss, summarize, and classify the meta-heuristic approaches algorithm applications for PV parameter identification introduced in this paper. In general, the summary is mainly based on year of application, utilized model, applied approaches, number of identified parameters, used data, advantages and disadvantages of various strategies, and type of PV cells.

5.2. Application of meta-heuristic algorithms on PV cell efficiency improvement

Note that the aforementioned meta-heuristic algorithms can not only be utilized in parameter identification of PV cells, but can also be applied on MPPT of PV systems under partial shading conditions (PSC) [151,152], which is crucial for the improvement of PV cell efficiency in practical engineering applications. Compared with conventional MPPT algorithms, such as perturb & observe (P&O) [153], meta-heuristic algorithms can often achieve more desirable results. Particularly, in order to more explicitly compare the specific performance of various MPPT techniques, a series of representative algorithms are tabulated in Table 22 to undertake a systematic summary based on their publication year, complexity level, tracking speed, efficiency, and DC-DC converter, etc. Moreover, since not all the aforementioned algorithms have been applied on MPPT and the efficiency of several algorithms are not specified in references, the algorithms are arranged in chronological order instead of being further classified.

Apart from various existing single meta-heuristic algorithms, hybrid algorithms which combine the merits of various individual algorithms should be more emphasized due to they can often acquire quite satisfactory results in MPPT under PSC. Besides, hardware experiments should be undertaken to further verify the MPPT performance of various algorithms, which can more accurately reflect the implementation feasibility of these methods in practical applications.

6. Conclusion

This paper undertakes a comprehensive review of various state-of-the-art meta-heuristic algorithms applied on PV cell parameter identification, which has put great emphasis on the basic theory and the experimental performance of each approach. Furthermore, a comprehensive summary of various meta-algorithms is tabulated to more specifically summarize the characteristics and features of these methods. The main contributions/recommendations can be summarized as follows:

a) The concept, main advantages and disadvantages of each algorithm for PV cell parameter identification are analyzed, especially in terms of the application accuracy, convergence speed, and practicability.

Compared with previous reviews on such field, this paper has greatly enriched the diversity of algorithms, the simulated results and the comparison of various algorithms. Hence, improved and modified variants can be further proposed based on these analyses to effectively improve existing methods;

b) The advantages of various algorithms for PV cell parameter identification need to be sufficiently utilized, such as SA is basically not influenced by the variation of irradiation level. Through efficiently combining and utilizing the merits of different approaches, some novel hybrid methods can be developed and applied to achieve more desirable results;
c) It is noteworthy that the PV cell parameters provided by manufacturers or experiments are usually tested under STC, while the practical operation conditions can barely maintain at STC. Hence, for the sake of verifying the practical performance of the algorithms, the experiments require to be carried out under various operation conditions;
d) Various PV cells/modules utilized for parameter identification are also introduced, while the PV cell models also need to be further improved rather than only those traditional models. In particular, novel PV cell models need to be established to combine with new approaches for better performance, especially for highly sensitive applications.

Declaration of Competing Interest

The authors declare that they have no known competing financial interests or personal relationships that could have appeared to influence the work reported in this paper.

Acknowledgments

The authors gratefully acknowledge the support of National Natural Science Foundation of China (61963020, 51907112, 51777078, 51977102), the Fundamental Research Funds for the Central Universities (D2172920), the Key Projects of Basic Research and Applied Basic Research in Universities of Guangdong Province (2018KZDXM001), Natural Science Foundation of Guangdong Province of China (2019A1515011671), Research and Development Start-Up Foundation of Shantou University (NTF19001), and the Science and Technology Projects of China Southern Power Grid (GDKJXM20172831).

References

[1] Liao SW, Yao W, Han XN, Wen JY, Cheng SJ. Chronological operation simulation framework for regional power system under high penetration of renewable energy using meteorological data. Appl Energy 2017;203:816–28.
[2] Yang B, Yu T, Shu HC, Dong J, Jiang L. Robust sliding-mode control of wind energy conversion systems for optimal power extraction via nonlinear perturbation observers. Appl Energy 2018;210:711–23.
[3] Yang B, Yu T, Shu HC, Zhang YM, Chen J, Sang YY, et al. Passivity-based sliding-mode control design for optimal power extraction of a PMSG based variable speed wind turbine. Renewable Energy 2018;119:577–89.
[4] Liu J, Wen JY, Yao W, Long Y. Solution to short-term frequency response of wind farms by using energy storage systems. IET Renew Power Gener 2016;10(5):669–78.
[5] Liu J, Yao W, Wen JY, Fang JK, Jiang L, He HB, et al. Impact of power grid strength and PLL parameters on stability of grid-connected DFIG wind farm. IEEE Trans Sustainable Energy 2019. https://doi.org/10.1109/TSTE.2019.2897596.
[6] Li GD, Li GY, Zhou M. Model and application of renewable energy accommodation capacity calculation considering utilization level of interprovincial tie-line. Protect Control Modern Power Syst 2019;4(4):1–12.
[7] Cv V, Kamaraj N. Modeling and performance analysis of the solar photovoltaic cell model using embedded MATLAB. Simulat: Trans Soc Model Simulat Int 2015;91(3):217–32.
[8] Humada AM, Hojabri M, Mekhilef S, Hamada HM. Solar cell parameters extraction based on single and double-diode models: A review. Renew Sustain Energy Rev 2016;56:494–509.
[9] Abbassi A, Gammoudi R, Dami MA, Hasnaoui O, Jemli M. An improved single-diode model parameters extraction at different operating conditions with a view to modeling a photovoltaic generator: A comparative study. Sol Energy 2017;155:478–89.
[10] Abbassi R, Abbassi A, Jemli M, Chebbi S. Identification of unknown parameters of solar cell models: A comprehensive overview of available approaches. Renew Sustain Energy Rev 2018;90:453–74.
[11] Khanna V, Das BK, Bisht D, Vandana Singh PK. A three diode model for industrial solar cells and estimation of solar cell parameters using PSO algorithm. Renewable Energy 2015;78:105–13.
[12] Allam D, Yousri DA, Eteiba MB. Parameters extraction of the three diode model for the multi-crystalline solar cell/module using Moth-Flame optimization algorithm. Energy Convers Manage 2016;123:535–48.
[13] Zhang DL, Li JL, Hui D. Coordinated control for voltage regulation of distribution network voltage regulation by distributed energy storage systems. Protect Control Modern Power Syst 2018;3(3). https://doi.org/10.1186/s41601-018-0077-1.
[14] Murty VVSN, Kumar A. Multi-objective energy management in microgrids with hybrid energy sources and battery energy storage systems. Protect Control Modern Power Syst 2020;5(2). https://doi.org/10.1186/s41601-019-0147-z.
[15] Yang B, Jiang L, Wang L, Yao W, Wu QH. Nonlinear maximum power point tracking control and model analysis of DFIG based wind turbine. Int J Electr Power Energy Syst 2016;74:429–36.
[16] Chen J, Yao W, Zhang CK, Ren Y, Jiang L. Design of robust MPPT controller for grid-connected PMSG-Based wind turbine via perturbation observation based nonlinear adaptive control. Renewable Energy 2019;134:478–95.
[17] Jordehi AR. Parameter estimation of solar photovoltaic (PV) cells: A review. Renew Sustain Energy Rev 2016;61:354–71.
[18] Chegaar M, Ouennoughi Z, Guechi F. Extracting dc parameters of solar cells under illumination. Vacuum 2004;75(4):367–72.
[19] Chin VJ, Salam Z, Ishaque K. Cell modelling and model parameters estimation techniques for photovoltaic simulator application: A review. Appl Energy 2015;154:500–19.
[20] Bai JB, Liu S, Hao YZ, Zhang Z, Jiang M, Zhang Y. Development of a new compound method to extract the five parameters of PV modules. Energy Convers Manage 2014;79:294–303.
[21] Appelbaum J, Peled A. Parameters extraction of solar cells-A comparative examination of three methods. Sol Energy Mater Sol Cells 2014;122:164–73.
[22] Dabra V, Paliwal KK, Sharma P, Kumar N. Optimization of photovoltaic power system: a comparative study. Protect Control Modern Power Syst 2017;2(2):29–39.
[23] Chan DSH, Phang JCH. Analytical methods for the extraction of solar-cell single- and double-diode model parameters from *I-V* characteristics. IEEE Trans Electron Dev 1987;34(2):286–93.
[24] Zhang ZZ, Ji J, Cheng XF, Zeng L. Universal analytical solution to the optimum load of the solar cell. Renewable Energy 2015;83:55–60.
[25] Torabi KE, Eddine IA, Obbadi A, Errami A, Rmaily R, Sahnoun S, et al. Parameters estimation of the single and double diode photovoltaic models using a Gauss-Seidel algorithm and analytical method: A comparative study. Energy Convers Manage 2017;148:1041–54.
[26] Roeva O, Fidanova S. Comparison of different metaheuristic algorithms based on intercriteria analysis. J Comput Appl Math 2018;340:615–28.
[27] Mahdavi S, Shiri ME, Rahnamayan S. Metaheuristics in large-scale global continues optimization: A survey. Inf Sci 2015;295:407–28.
[28] Majdoul R, Abdelmounim E, Aboulfatah M, Touati AW, Moutabir A, Abouloifa A. Combined analytical and numerical approach to determine the four parameters of the photovoltaic cells models. International Conference on Electrical and Information Technologies, March 2015, Marrakech, Morocco. 2015. p. 263–8.
[29] Kamali SK, Rahim NA, Mokhlis H, Tyagi VV. Photovoltaic electricity generator dynamic modeling methods for smart grid applications: A review. Renew Sustain Energy Rev 2016;57:131–72.
[30] Kumar M, Kumar A. An efficient parameters extraction technique of photovoltaic models for performance assessment. Sol Energy 2017;158:192–206.
[31] Wolf P, Benda V. Identification of PV solar cells and modules parameters by combining statistical and analytical methods. Sol Energy 2013;93:151–7.
[32] Pillai DS, Rajasekar N. Metaheuristic algorithms for PV parameter identification: A comprehensive review with an application to threshold setting for fault detection in PV systems. Renew Sustain Energy Rev 2018;82(3):3503–25.
[33] Nesmachnow S. An overview of metaheuristics: accurate and efficient methods for optimization. Int J Metaheuristics 2014;3(4):320–47.
[34] Fathy A. Recent meta-heuristic grasshopper optimization algorithm for optimal reconfiguration of partially shaded PV array. Sol Energy 2018;171:638–51.
[35] Ishaque K, Salam Z. An improved modeling method to determine the model parameters of photovoltaic (PV) modules using differential evolution (DE). Sol Energy 2011;85(9):2349–59.
[36] Mi Z, Chen JK, Chen NF, Bai YM, Fu R, Liu H. Open-loop solar tracking strategy for high concentrating photovoltaic systems using variable tracking frequency. Energy Convers Manage 2016;117:142–9.
[37] Chander S, Purohit A, Sharma A, Nehra SP, Dhaka MS. Impact of temperature on performance of series and parallel connected mono-crystalline silicon solar cells. Energy Rep 2015;1:175–80.
[38] Masuko K, Shigematsu M, Hashiguchi T, Fujishima D, Kai M, Yoshimura N, et al. Achievement of more than 25% conversion efficiency with crystalline silicon heterojunction solar cell. IEEE J Photovoltaics 2014;4(6):1433–5.
[39] Micheli D, Alessandrini S, Radu R, Casula I. Analysis of the outdoor performance and efficiency of two grid connected photovoltaic systems in northern Italy. Energy Convers Manage 2014;80:436–45.
[40] Schindlera F, Fella A, Müllera R, Benicka J, Richtera A, Feldmanna F, et al. Towards the efficiency limits of multicrystalline silicon solar cells. Sol Energy Mater Sol Cells 2018;185:198–204.
[41] Tripathi B, Yadav P, Rathod S, Kumar M. Performance analysis and comparison of

two silicon material based photovoltaic technologies under actual climatic conditions in Western India. Energy Convers Manage 2014;80:97–102.
[42] Tihane A, Boulaid M, Elfanaoui A, Nya M, Ihlal A. Performance analysis of mono and poly-crystalline silicon photovoltaic modules under Agadir climatic conditions in Morocco. Mater Today: Proc 2019. https://doi.org/10.1016/j.matpr.2019.07.620.
[43] Cao Y, Zhu XY, Chen HB, Zhang XT, Zhou J, Hu ZY, et al. Towards high efficiency inverted Sb2Se3 thin film solar cells. Sol Energy Mater Sol Cells 2019, 200.. https://doi.org/10.1016/j.solmat.2019.109945.
[44] Fuentealba E, Ferrada P, Araya F, Marzo A, Parrado C, Portillo C. Photovoltaic performance and LCoE comparison at the coastal zone of the Atacama Desert, Chile. Energy Convers Manage 2015;95:181–6.
[45] Bianchini A, Gambuti M, Pellegrini M, Saccani C. Performance analysis and economic assessment of different photovoltaic technologies based on experimental measurements. Renewable Energy 2016;85:1–11.
[46] Romero JM, Almonacid F, Theristis M, Casa J, Georghiou GE, Fernández EF. Comparative analysis of parameter extraction techniques for the electrical characterization of multi-junction CPV and m-Si technologies. Sol Energy 2018;160:275–88.
[47] Lim LH, Ye Z, Ye JY, Yang DZ, Du H. A linear method to extract diode model parameters of solar panels from a single *I-V* curve. Renewable Energy 2015;76:135–42.
[48] Ishaque K, Salam Z, Taheri H, Shamsudin A. A critical evaluation of EA computational methods for photovoltaic cell parameter extraction based on two diode model. Sol Energy 2011;85(9):1768–79.
[49] Macabebe EQB, Sheppard CJ, Dyk E. Parameter extraction from *I-V* characteristics of PV devices. Sol Energy 2011;85(1):12–8.
[50] Ram JP, Manghani Manghani H, Pillai DS, Babu TS, Miyatake M, Rajasekara N. Analysis on solar PV emulators: A review. Renew Sustain Energy Rev 2018;81:149–60.
[51] Mares Oana, Paulescu M, Badescu V. A simple but accurate procedure for solving the five-parameter model. Energy Convers Manage 2015;105:139–48.
[52] Nagayoshi H, Orio S, Kono Y, Nakajima H. Novel PV array/module I-V curve simulator circuit. Conference Record of the Twenty-Ninth IEEE Photovoltaic Specialists Conference, 19-24 May 2002, New Orleans, LA, USA. 2002. p. 1535–8.
[53] Ishaque K, Salam Z, Syafaruddin. A comprehensive MATLAB Simulink PV system simulator with partial shading capability based on two-diode model. Sol Energy 2011;85(9):2217–27.
[54] Ma T, Yang HX, Lu L. Development of a model to simulate the performance characteristics of crystalline silicon photovoltaic modules/strings/arrays. Sol Energy 2014;100:31–41.
[55] Hejri M, Mokhtari H, Azizian MZ, Ghandhari M, Soder L. On the parameter extraction of a five-parameter double-diode model of photovoltaic cells and modules. IEEE J Photovoltaics 2014;4(3):915–23.
[56] Qais MH, Hasanien HM, Alghuwainem S. Identification of electrical parameters for three-diode photovoltaic model using analytical and sunflower optimization algorithm. Appl Energy 2019;250:109–17.
[57] Muhsen DH, Ghazali AB, Khatib T, Abed IA. Parameters extraction of double diode photovoltaic module's model based on hybrid evolutionary algorithm. Energy Convers Manage 2015;105:552–61.
[58] Moshksar E, Ghanbari T. Adaptive estimation approach for parameter identification of photovoltaic modules. IEEE J Photovoltaics 2017;7(2):614–23.
[59] Silva EA, Bradaschia F, Cavalcanti MC, Nascimento AJ. Parameter estimation method to improve the accuracy of photovoltaic electrical model. IEEE J Photovoltaics 2016;6(1):278–85.
[60] Tong NT, Pora W. A parameter extraction technique exploiting intrinsic properties of solar cells. Appl Energy 2016;176:104–15.
[61] Gomes RCM, Vitorino MA, Correa MBR, Fernandes DA, Wang RX. Shuffled complex evolution on photovoltaic parameter extraction: A comparative analysis. IEEE Trans Sustainable Energy 2017;8(2):805–15.
[62] Rajasekar N, Kumar NK, Venugopalan N. Bacterial foraging algorithm based solar PV parameter estimation. Sol Energy 2013;97:255–65.
[63] Babu TS, Ram JP, Sangeetha K, Laudani A, Rajasekar N. Parameter extraction of two diode solar PV model using fireworks algorithm. Sol Energy 2016;140:265–86.
[64] Askarzadeh A, Rezazadeh A. Parameter identification for solar cell models using harmony search-based algorithms. Sol Energy 2012;86(11):3241–9.
[65] Kler D, Sharma P, Banerjee A, Rana KPS, Kumar V. PV cell and module efficient parameters estimation using evaporation rate based water cycle algorithm. Swarm Evol Comput 2017;35:93–110.
[66] Ayodele TR, Ogunjuyigbe ASO, Ekoh EE. Evaluation of numerical algorithms used in extracting the parameters of a single-diode photovoltaic model. Sustainable Energy Technol Assess 2016;13:51–9.
[67] Zagrouba M, Sellami A, Bouaïcha M, Ksouri M. Identification of PV solar cells and modules parameters using the genetic algorithms: Application to maximum power extraction. Sol Energy 2010;84(5):860–6.
[68] Dizqah AM, Maheri A, Busawon K. An accurate method for the PV model identification based on a genetic algorithm and the interior-point method. Renewable Energy 2014;72:212–22.
[69] Jervase JA, Bourdoucen H, Al-lawati AM. Solar cell parameter extraction using genetic algorithms. Meas Sci Technol 2001;12:1922–5.
[70] Fathy A, Rezk H. Parameter estimation of photovoltaic system using imperialist competitive algorithm. Renewable Energy 2017;111:307–20.
[71] Qais MH, Hasanien HM, Alghuwainem S, Nouh AS. Coyote optimization algorithm for parameters extraction of three-diode photovoltaic models of photovoltaic modules. Energy 2019;187. https://doi.org/10.1016/j.energy.2019.116001.
[72] Chaibi Y, Malvoni M, Allouhi A, Mohamed S. Data on the I-V characteristics related to the SM55 monocrystalline PV module at various solar irradiance and temperatures. Data in brief 2019;26. https://doi.org/10.1016/j.dib.2019.104527.
[73] Rodriguez JDB, Petrone G, Paja AR, Spagnuolo G. A genetic algorithm for identifying the single diode model parameters of a photovoltaic panel. Math Comput Simul 2017;134:38–54.
[74] Konak A, Coit DW, Smith AE. Multi-objective optimization using genetic algorithms: A tutorial. Reliab Eng Syst Saf 2006;91(9):992–1007.
[75] Ismail MS, Moghavvemi M, Mahlia TMI. Characterization of PV panel and global optimization of its model parameters using genetic algorithm. Energy Convers Manage 2013;73:10–25.
[76] Kumari PA, Geethanjali P. Adaptive genetic algorithm based multi-objective optimization for photovoltaic cell design parameter extraction. Energy Procedia 2017;117:432–41.
[77] Storn R, Price K. Differential evolution-a simple and efficient heuristic for global optimization over continuous spaces. J Global Optim 1997;11(4):341–59.
[78] Jiang LL, Maskell DL, Patra JC. Parameter estimation of solar cells and modules using an improved adaptive differential evolution algorithm. Appl Energy 2013;112:185–93.
[79] Gong WY, Cai ZH. Parameter extraction of solar cell models using repaired adaptive differential evolution. Sol Energy 2013;94:209–20.
[80] Ishaque K, Salam Z, Mekhilef S, Shamsudin A. Parameter extraction of solar photovoltaic modules using penalty-based differential evolution. Appl Energy 2012;99:297–308.
[81] Muhsenab DH, Ghazali AB, Khatib T, Abed IA. Extraction of photovoltaic module model's parameters using an improved hybrid differential evolution/electromagnetism-like algorithm. Sol Energy 2015;119:286–97.
[82] Muangkote N, Sunat K, Chiewchanwattana S, Kaiwinit S. An advanced onlooker-ranking-based adaptive differential evolution to extract the parameters of solar cell models. Renewable Energy 2019;134:1129–47.
[83] Askarzadeh A, Rezazadeh A. Artificial bee swarm optimization algorithm for parameters identification of solar cell models. Appl Energy 2013;102:943–9.
[84] Yang B, Yu T, Zhang XS, Li HF, Shu HC, Sang YY, et al. Dynamic leader based collective intelligence for maximum power point tracking of PV systems affected by partial shading condition. Energy Convers Manage 2019;179:286–303.
[85] Oliva D, Cuevas E, Pajares G. Parameter identification of solar cells using artificial bee colony optimization. Eenergy 2014;72:93–102.
[86] Wang RJ, Zhan YJ, Zhou HF. Application of artificial bee colony in model parameter identification of solar cells. Energies 2015;8(8):7563–81.
[87] Oliva D, Ewees AA, Elaziz MA, Hassanien E, Cisneros MP. A Chaotic improved artificial bee colony for parameter estimation of photovoltaic cells. Energies 2018;11(5):865–83.
[88] Chen X, Xu B, Mei CL, Ding YH, Li KJ. Teaching-learning-based artificial bee colony for solar photovoltaic parameter estimation. Appl Energy 2018;212:1578–88.
[89] Mirjalili S, Lewis A. The whale optimization algorithm. Adv Eng Softw 2016;95:51–67.
[90] Dasu B, Sivakumar M, Srinivasarao R. Interconnected multi-machine power system stabilizer design using whale optimization algorithm. Protect Control Modern Power Syst 2019;4(4):13–23.
[91] Amroune M, Bouktir T. Musirin I. Power system voltage instability risk mitigation via emergency demand response-based whale optimization algorithm. Protect Control Modern Power Syst 2019;4(25). https://doi.org/10.1186/s41601-019-0142-4.
[92] Elazab OS, Hasanien HM, Elgendy MA, Abdeen AM. Parameters estimation of single- and multiple-diode photovoltaic model using whale optimisation algorithm. IET Renew Power Gener 2018;12(15):1755–61.
[93] Xiong GJ, Zhang J, Shi DY, He Y. Parameter extraction of solar photovoltaic models using an improved whale optimization algorithm. Energy Convers Manage 2018;174:388–405.
[94] Oliva D, Elaziz MA, Hassanien A. Parameter estimation of photovoltaic cells using an improved chaotic whale optimization algorithm. Appl Energy 2017;200:141–54.
[95] Sun YJ, Wang XL, Chen YH, Liu ZJ. A modified whale optimization algorithm for large-scale global optimization problems. Expert Syst Appl 2018;114:563–77.
[96] Wu ZQ, Yu DQ, Kang XH. Parameter identification of photovoltaic cell model based on improved ant lion optimizer. Energy Convers Manage 2017;151:107–15.
[97] Simon D. Biogeography-based optimization. IEEE Trans Evol Comput 2008;12(6):702–13.
[98] Boussaïd I, Chatterjee A, Siarry M, Nacer MA. Biogeography-based optimization for constrained optimization problems. Renewable Energy 2012;39(12):3293–304.
[99] Niu Q, Zhang L, Li K. A biogeography-based optimization algorithm with mutation strategies for model parameter estimation of solar and fuel cells. Energy Convers Manage 2014;86:1173–85.
[100] Joshi AS, Kulkarni O, Kakandikar GM, Nandedkar VM. Cuckoo search optimization-A review. Mater Today 2017;4(8):7262–9.
[101] Kang T, Yao JG, Jin M, Yang SJ, Duong TL. A novel improved cuckoo search algorithm for parameter estimation of photovoltaic (PV) models. Energies 2018;11(5):1060–90.
[102] Ma JM, Ting TO, Man KL, Zhang N, Guan SU, Wong WH. Parameter estimation of photovoltaic models via cuckoo search. J Appl Math 2013(2). https://doi.org/10.1155/2013/362619.
[103] Chen X, Yu KJ. Hybridizing cuckoo search algorithm with biogeography-based optimization for estimating photovoltaic model parameters. Sol Energy 2019;180:192–206.
[104] Askarzadeh A, Rezazadeh A. Extraction of maximum power point in solar cells using bird mating optimizer-based parameters identification approach. Sol Energy

2013;90:123–33.
[105] Askarzadeh A, Coelho LS. Determination of photovoltaic modules parameters at different operating conditions using a novel bird mating optimizer approach. Energy Convers Manage 2015;89:608–14.
[106] Shang LQ, Zhu WW, Li PW, Guo HC. Maximum power point tracking of PV system under partial shading conditions through flower pollination algorithm. Protect Control Modern Power Syst 2018;3(3):400–6.
[107] Alam DF, Yousri DA, Eteiba MB. Flower pollination algorithm based solar PV parameter estimation. Energy Convers Manage 2015;101:410–22.
[108] Ram JP, Babu S, Dragicevic T, Rajasekar N. A new hybrid bee pollinator flower pollination algorithm for solar PV parameter estimation. Energy Convers Manage 2017;135:463–76.
[109] Yang B, Zhang XS, Yu T, Shu HC, Fang ZH. Grouped grey wolf optimizer for maximum power point tracking of doubly-fed induction generator based wind turbine. Energy Convers Manage 2017;133:427–43.
[110] Kamboj VK, Bath SK, Dhillon JS. Solution of non-convex economic load dispatch problem using grey wolf optimizer. Neural Comput Appl 2016;27(5):1301–16.
[111] Zhang S, Luo QF, Zhou YQ. Hybrid grey wolf optimizer using elite opposition-based learning strategy and simplex method. Int J Comput Intell Appl 2017. https://doi.org/10.1142/S1469026817500122.
[112] Nayak B, Mohapatra A, Mohanty KB. Parameter estimation of single diode PV module based on GWO algorithm. Renewable Energy Focus 2019;30:1–12.
[113] Passino KM. Biomimicry of bacterial foraging for distributed optimization and control. IEEE Control Syst Mag 2002;22(3):56–67.
[114] Awadallah MA. Variations of the bacterial foraging algorithm for the extraction of PV module parameters from nameplate data. Energy Convers Manage 2016;113:312–20.
[115] Diabat A, Kannan D, Kaliyan M, Svetinovic D. An optimization model for product returns using genetic algorithms and artificial immune system. Resour Conserv Recycl 2013;74:156–69.
[116] Jacob B, Balasubramanian K, Babu TS, Azharuddin SM, Rajasekar N. Solar PV modelling and parameter extraction using artificial immune system. Energy Procedia 2015;75:331–6.
[117] Yang B, Zhong LE, Yu T, Li HF, Zhang XS, Shu HC, et al. Novel bio-inspired memetic salp swarm algorithm and application to MPPT for PV systems considering partial shading condition. J Cleaner Prod 2019;215:1203–22.
[118] Mirjalili S, Gandomi AH, Mirjalili SZ, Saremi S, Faris H, Mirjalili SM. Salp swarm algorithm: a bio-inspired optimizer for engineering design problems. Adv Eng Softw 2017;114:163–91.
[119] Abbassi R, Abbassi A, Heidari AA, Mirjalili S. An efficient salp swarm-inspired algorithm for parameters identification of photovoltaic cell models. Energy Convers Manage 2019;179:362–72.
[120] Del Valle Y, Venayagamoorthy GK, Mohagheghi S, Hernandez JC, Harley RG. Particle swarm optimization: basic concepts, variants and applications in power systems. IEEE Trans Evol Comput 2008;12(2):171–95.
[121] Ye MY, Wang XD, Xu YS. Parameter extraction of solar cells using particle swarm optimization. J Appl Phys 2009;105(9). 094502-094502-8.
[122] Injeti SK, Thunuguntla VK. Optimal integration of DGs into radial distribution network in the presence of plug-in electric vehicles to minimize daily active power losses and to improve the voltage profile of the system using bio-inspired optimization algorithms. Protect Control Modern Power Syst 2020;5(3). https://doi.org/10.1186/s41601-019-0149-x.
[123] Elsheikh AH, Elaziz MA. Review on applications of particle swarm optimization in solar energy systems. Int J Environ Sci Technol 2019;16(2):1159–70.
[124] Ebrahimi SM, Salahshour E, Malekzadeh M, Gordillo F. Parameters identification of PV solar cells and modules using flexible particle swarm optimization algorithm. Energy 2016;140:265–76.
[125] Nunes HGG, Pombo JAN, Mariano SJPS, Calado MRA, Felippe de Souza JAM. A new high performance method for determining the parameters of PV cells and modules based on guaranteed convergence particle swarm optimization. Appl Energy 2018;211:774–91.
[126] Ma JM, Man KL, Guan SU, Ting TO, Wong WH. Parameter estimation of photovoltaic model via parallel particle swarm optimization algorithm. Int J Energy Res 2015;40(3):343–52.
[127] Jordehi AR. Time varying acceleration coefficients particle swarm optimisation (TVACPSO): A new optimisation algorithm for estimating parameters of PV cells and modules. Energy Convers Manage 2016;129:262–74.
[128] Jordehi AR. Enhanced leader particle swarm optimisation (ELPSO): An efficient algorithm for parameter estimation of photovoltaic (PV) cells and modules. Sol Energy 2018;159:78–87.
[129] Yuan X, Yang Y, Wang H. Improved parallel chaos optimization algorithm. Appl Math Comput 2012;219(8):3590–9.
[130] Yuan XF, Xiang YZ, He YQ. Parameter extraction of solar cell models using mutative-scale parallel chaos optimization algorithm. Sol Energy 2014;108:238–51.
[131] El-Naggar KM, AlRashidi MR, AlHajri MF, Al-Othman AK. Simulated annealing algorithm for photovoltaic parameters identification. Sol Energy 2012;86(1):266–74.
[132] Dkhichi F, Oukarfi B, Fakkar A, Belbounaguia N. Parameter identification of solar cell model using Levenberg-Marquardt algorithm combined with simulated annealing. Sol Energy 2014;110:781–8.
[133] Shen Y, Yao W, Wen JY, He HB, Jiang L. Resilient wide-area damping control using GrHDP to tolerate communication failures. IEEE Trans Smart Grid 2019;10(3):2547–57.
[134] Bayraktar Z, Komurcu M, Bossard JA, Werner DH. The wind driven optimization technique and its application in electromagnetics. IEEE Trans Antennas Propag 2013;61(5):2745–57.
[135] Derick M, Rani C, Rajesh M, Farrag ME, Wang Y, Busawon K. An improved optimization technique for estimation of solar photovoltaic parameters. Sol Energy 2017;157:116–24.
[136] Sadollah A, Eskandar H, Bahreininejad A, Kim JH. Water cycle algorithm with evaporation rate for solving constrained and unconstrained optimization problems. Appl Soft Comput 2017;30:58–71.
[137] Pourmousa N, Ebrahimi SM, Malekzadeh M, Alizadeh M. Parameter estimation of photovoltaic cells using improved Lozi map based chaotic optimization algorithm. Sol Energy 2019;180:180–91.
[138] Yuan X, Zhao J, Yang Y, Wang Y. Hybrid parallel chaos optimization algorithm with harmony search algorithm. Appl Soft Comput 2014;17:12–22.
[139] Patel SKJ, Panchal AK, Kheraj V. Extraction of solar cell parameters from a single current-voltage characteristic using teaching learning based optimization algorithm. Appl Energy 2014;119:384–93.
[140] Niu Q, Zhang HY, Li K. An improved TLBO with elite strategy for parameters identification of PEM fuel cell and solar cell models. Int J Hydrogen Energy 2014;39(8):3837–54.
[141] Chen X, Yu KJ, Du WL, Zhao WX, Liu GH. Parameters identification of solar cell models using generalized oppositional teaching learning based optimization. Energy 2016;99:170–80.
[142] Yu KJ, Liang JJ, Qu BY, Cheng ZP, Wang HS. Multiple learning backtracking search algorithm for estimating parameters of photovoltaic models. Appl Energy 2018;226:408–22.
[143] AlRashidi MR, AlHajri MF, El-Naggar KM, Al-Othman AK. A new estimation approach for determining the *I-V* characteristics of solar cells. Sol Energy 2011;85(7):1543–11450.
[144] Beigi AM, Maroosi A. Parameter identification for solar cells and module using a hybrid firefly and pattern search algorithms. Sol Energy 2018;171:435–46.
[145] AlHajri MF, El-Naggar KM, AlRashidi MR, Al-Othman AK. Optimal extraction of solar cell parameters using pattern search. Renewable Energy 2012;44:238–45.
[146] Gao XK, Cui Y, Hu JJ, Xu GY, Wang ZF, Qu JH, et al. Parameter extraction of solar cell models using improved shuffled complex evolution algorithm. Energy Convers Manage 2018;157:460–79.
[147] Chen YX, Chen ZC, Wu LJ, Long C, Lin PJ, Cheng SY. Parameter extraction of PV models using an enhanced shuffled complex evolution algorithm improved by opposition-based learning. Energy Procedia 2019;158:991–7.
[148] Yu KJ, Liang JJ, Qu BY, Chen X, Wang HS. Parameters identification of photovoltaic models using an improved JAYA optimization algorithm. Energy Convers Manage 2017;150:742–53.
[149] Yu KJ, Qu BY, Yue CT, Ge SL, Chen X, Liang J. A performance-guided JAYA algorithm for parameters identification of photovoltaic cell and module. Appl Energy 2019;237:241–57.
[150] Wang L, Huang C. A novel elite opposition-based Jaya algorithm for parameter estimation of photovoltaic cell models. Optik 2018;155:351–6.
[151] Chaibi Y, Allouhi A, Salhi M, El-jouni A. Annual performance analysis of different maximum power point tracking techniques used in photovoltaic systems. Protect Control Modern Power Syst 2019;4(4):171–80.
[152] Hamdi H, Regaya CB, Zaafouri A. A sliding-neural network control of induction-motor-pump supplied by photovoltaic generator. Protect Control Modern Power Syst 2019;4(4):306–22.
[153] Salman S, Xin AI, Zhouyang WU. Design of a P-&-O algorithm based MPPT charge controller for a stand-alone 200W PV system. Protect Control Modern Power Syst 2018;3(3):259–66.
[154] Daraban S, Petreus D, Morel C. A novel MPPT algorithm based on a modified genetic algorithm specialized on tracking the global maximum power point in photovoltaic systems affected by partial shading. Energy 2014;74:374–88.
[155] Tajuddin MFN, Ayob SM, Salam Z. Global maximum power point tracking of PV system using dynamic population size differential evolution (DynNP-DE) algorithm. 2014 IEEE Conference on Energy Conversion (CENCON). 13-14 October 2014, Johor Bahru, Malaysia. 2014. p. 254–9.
[156] Lyden S, Haque ME. A simulated annealing global maximum power point tracking approach for PV modules under partial shading conditions. IEEE Trans Power Electron 2015;31(6):4171–81.
[157] Mohanty S, Subudhi B, Ray PK. A grey wolf-assisted perturb & observe MPPT algorithm for a PV system. IEEE Trans Energy Convers 2016;32(1):340–7.
[158] Kumar CS, Rao RS. A novel global MPP tracking of photovoltaic system based on whale optimization algorithm. Int J Renewable Energy Dev 2016;5(3):225–32.
[159] Javed MY, Murtaza AF, Ling Q, Qamar S, Gulzar MM. A novel MPPT design using generalized pattern search for partial shading. Energy Build 2016;133:59–69.
[160] Karatepe E, Hiyama T. Performance enhancement of photovoltaic array through string and central based MPPT system under non-uniform irradiance conditions. Energy Convers Manage 2012;62:131–40.
[161] Cherukuri SK, Rayapudi SR. Enhanced grey wolf optimizer based MPPT algorithm of PV system under partial shaded condition. Int J Renewable Energy Dev 2017;6(3):203–12.
[162] Ram JP, Rajasekar N. A new robust, mutated and fast tracking LPSO method for solar PV maximum power point tracking under partial shaded conditions. Appl Energy 2017;201:45–59.
[163] Sen T, Pragallapati N, Agarwal V, Kumar R. Global maximum power point tracking of PV arrays under partial shading conditions using a modified particle velocity-based PSO technique. IET Renew Power Gener 2017;12(5):555–64.
[164] Tobón A, Peláez-Restrepo J, Villegas-Ceballos J, Serna-Garcés S, Herrera J, Ibeas A. Maximum power point tracking of photovoltaic panels by using improved pattern search methods. Energies 2017;10(9):1316–30.
[165] Huang YP, Chen X, Ye CE. A hybrid maximum power point tracking approach for photovoltaic systems under partial shading conditions using a modified genetic

algorithm and the firefly algorithm. Int J Photoenergy 2018. https://doi.org/10.1155/2018/7598653.
[166] Pei T, Hao X, Gu Q. A novel global maximum power point tracking strategy based on modified flower pollination algorithm for photovoltaic systems under non-uniform irradiation and temperature conditions. Energies 2018;11(10):2708–25.
[167] Tey KS, Mekhilef S, Seyedmahmoudian M, Horan B, Oo AT, Stojcevski A. Improved differential evolution-based MPPT algorithm using SEPIC for PV systems under partial shading conditions and load variation. IEEE Trans Ind Inf 2018;14(10):4322–33.
[168] Abdalla O, Rezk H, Ahmed EM. Wind driven optimization algorithm based global MPPT for PV system under non-uniform solar irradiance. Sol Energy 2019;180:429–44.